LASER INTERFEROMETER GRAVITATIONAL WAVE OBSERVATORY

LIGO Laboratory / LIGO Scientific Collaboration

LIGO-T1000340-v1 *LIGO* March 20, 2010

Tiltmeter Characterization

Amanda O'Toole, Abhik Bhawal, Morgan Asadoor, Riccardo DeSalvo

Distribution of this document:
LIGO Scientific Collaboration

This is an internal working note
of the LIGO Laboratory.

California Institute of Technology
LIGO Project – MS 18-34
1200 E. California Blvd.
Pasadena, CA 91125
Phone (626) 395-2129
Fax (626) 304-9834
E-mail: info@ligo.caltech.edu

Massachusetts Institute of Technology
LIGO Project – NW22-295
185 Albany St
Cambridge, MA 02139
Phone (617) 253-4824
Fax (617) 253-7014
E-mail: info@ligo.mit.edu

LIGO Hanford Observatory
P.O. Box 1970
Richland WA 99352
Phone 509-372-8106
Fax 509-372-8137

LIGO Livingston Observatory
P.O. Box 940
Livingston, LA 70754
Phone 225-686-3100
Fax 225-686-7189

http://www.ligo.caltech.edu/

Table of Contents

1 Introduction and Tiltmeter Overview

The purpose of testing this prototype of a new kind of tiltmeter was to characterize its properties such as hysteresis, noise, and effects of changing the natural frequency. The tiltmeter is composed of a massive arm pivoting on a knife-edge or a flexure. Presently we use a knife-edge made of roughly cut tungsten carbide. Below each end of the arm is a coil actuator, which can dynamically change the equilibrium position of the tiltmeter. At each end of the arm are threaded holes above and below the pivot point where tuning masses can be placed. Adding mass below the pivot point lowers its center of mass, stabilizes the system, and increases the natural resonant frequency of the tiltmeter. Lastly, there is a pair of LVDT (Linear Variable Differential Transformer) position sensors above the arm on each end. The LVDT resolution is about a nanometer. The tiltmeter restoring force is mainly gravitational, due to the fact that the tiltmeter arm center of mass is slightly below the pivot point. The restoring torque is therefore the mass of the arm times Earth's gravity acceleration g times h times sin(θ).

$T_{gray} = M\ g\ h\ \sin(\theta) = K_{gray}\ \theta$

The momentum of inertia of the arm (given in figure) is 31191 x 10^-6 kgm.

A small tuning mass (a small washer) above the arm is used to balance the arm.

ASS6-bis: I1=1092,103 - I2=31015,423 - I3=31190,682

A model drawing of the flexure version of the tiltmeter arm. Here the masses are placed above the pivot point.

The tiltmeter control program (designed in Lab View) consists of multiple controls that are used to move the system and do such tasks as centering the equilibrium to a desired tilt, changing the strength of the resonant frequency, or simply giving oscillation-inducing kicks or slow sine-wave steps to measure hysteresis.

The program consists of a slow feedback section called the Integrator, which compared the actual with the desired tilt and centers the equilibrium point of the system on the chosen LVDT

position measurement (usually zero). The actuator coils are wound in opposite directions and wired in series. A quasi-static current given to the coils applies opposite forces to the tiltmeter ends, bringing it to the desired position. The "working point integrator" keeps track of the total amount the system has moved since original resting position. A parameter can be used to control the integrator response time at which the system is brought to the chosen equilibrium position. Because the integrator operated through a Digital to Analog Converter (DAC), which functions in finite steps, this introduced a problem that was noticed when looking at overnight data. Instead of the intended quiet operation, the tiltmeter was undergoing small jumps followed by ringdown oscillations throughout the night. The jerks are produced by the integrator at work. The graph below depicts the LVDT data centered at zero of an overnight run. Each jump and subsequent ringdown indicates a DAC change by one bit.

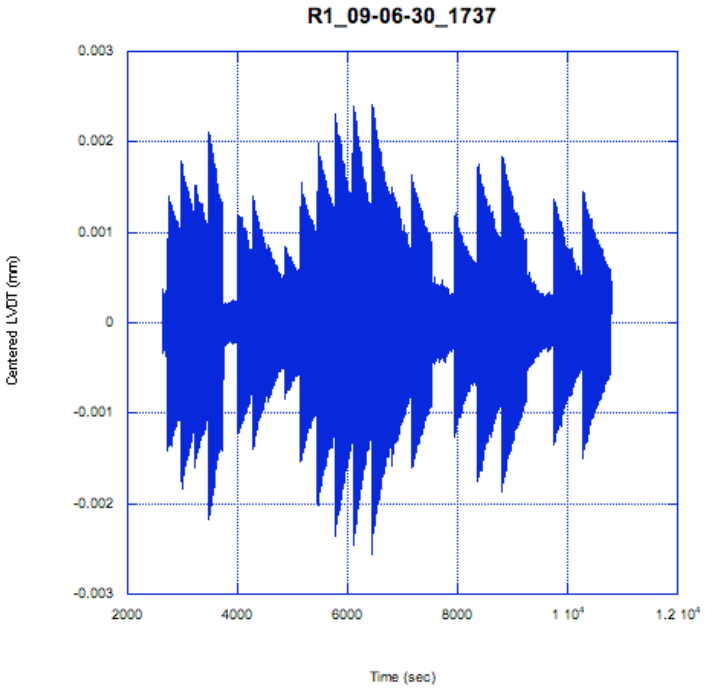

The noise introduced from the Integrator steps amounted to about 0.002 mm of movement. Because of this, an Integrator Pause was added to the system, which stopped the Integrator from continuously readjusting the position of the tiltmeter after the desired equilibrium point is reached. When in pause, only a constant current holding the system at the necessary working point is maintained.

2 Testing the Electro-Magnetic Anti-Spring

The tiltmeter control program was designed to change the effective stiffness coefficient $k_{eff} = k_{gray} + k_{EMAS}$ of the spring-like oscillations of the tiltmeter by introducing a tunable stiffness using the Electro-Magnetic Anti-Spring (EMAS) mechanism. The EMAS section introduces opposite forces on the actuator coils, a pure torque, which is proportional to the angular displacement from the equilibrium point (usually corresponding to $\theta=0$). This is equivalent to an elastic restoring torque, whose strength is tuned with the parameter called "EMAS" in the Labview-based control program.

The program uses two ADC converters to continually measure the angular position θ of the balance arm. The angle is measured using the difference of the two LVDTs on the two sides, above the balance arm. The LVDTs are calibrated in mm, to have the actual angle θ in radians, one needs to divide by the actual LVDT lever arm (125 mm). The EMAS part of the routine actually uses the raw LVDT output (in mm), multiplies it by the EMAS parameter, divide it by 10 and, through a DAC, generates an output voltage.
V_{out} = LVDT * EMAS /10
This voltage is fed to a current amplifier, with a gain of 10, which feeds the two actuator coils mounted below the balance arm. Therefore the net voltage on the coils will be
V_{coil} = LVDT * EMAS
The two coils are identical, wired in series, so that they will apply a net torque on the system.
$T_{EMAS} = K_{EMAS}\,\theta$ = G * EMAS * L * LVDT / L = G * EMAS * LVDT
Where G is the coil electrical gain in N/V. The gain G is calculated below.
Therefore K_{EMAS} = G * EMAS
The torque is stabilizing when EMAS is positive.

The lower the EMAS value, the less stable the system (an excess of EMAS gain makes it unstable, which causes the arm to rotate to one of the end points, half a mm away).
Because $k_{eff} = k_{gray} + k_{EMAS}$, changing the EMAS is supposedly equivalent to moving the masses on the arm of the tiltmeter so that they are higher or lower than the pivot point. This effectively changes the effective restoring force, thus changing the frequency of oscillation.
We expect that a graph of frequency versus k_{EMAS} would follow the equation $\omega = \sqrt{(k_{eff}/I)}$, fitting with the formula m2*sqrt(x-m1). The intercept m1 corresponds to the EMAS generating Keff = 0 and M2 is proportional to G, therefore we can obtain both k_{gray} and G. The frequency ω is the square root of the spring constant of the system divided by the mass, which in our system does not change. The spring constant is proportional to the EMAS gain, thus making the EMAS vs. frequency graph a square-root function.

After making tests and collecting data, we also wanted to analyze the frequency vs. the quality factor Q of the system.

2.1 Calculation of G

To measure the conversion constant G, we changed mechanically the equilibrium position of the tiltmeter by a known amount, i.e. by placing a small washer of mass 0.3849 g at 84 mm to the left of the pivot point. The coils are each 125 mm on either side of the pivot point. We left the

integrator on. When adding the washer, the voltage in the coil drivers keeping the system to its center position changed from -0.416 V to 7.688 V. We calculated the force applied on the system by the washer (3.722e-03 Newtons). Then, by taking into consideration the change in voltage, I determined the Newtons per Volt calibration constant for the coil to be 3.1278e-04 N/V (or 3197 V/N) for any force put on the coil.

2.2 Negative values of EMAS

We changed the EMAS values typically in steps of 0.1, starting from 0 and going down to the limiting value -2.70.
At each EMAS value we kicked the tiltmeter, then fitting the resulting ringdown data with the curve described by the function of the Kaleidagraph form

$$y = m4+m1*\sin(2*pi*(x-cmin(c0)-m2)*m3)*\exp(-(x-cmin(c0)-m2)/m5)$$

in more mathematical form

$$y=c+A\ \sin(2\pi f(t-t_2))\ e^{-(t-t_0)/\tau}$$

which allows us to determine the frequency f (m3), lifetime τ (m5), and Q-factor f*τ*π, and offset from zero. The graph of frequency and EMAS fit the square-root prediction quite accurately, with only a few slightly outlying points identified as payload resonances.
Curve fit: m2*sqrt(x-m1) with starting points m1=-2.7.

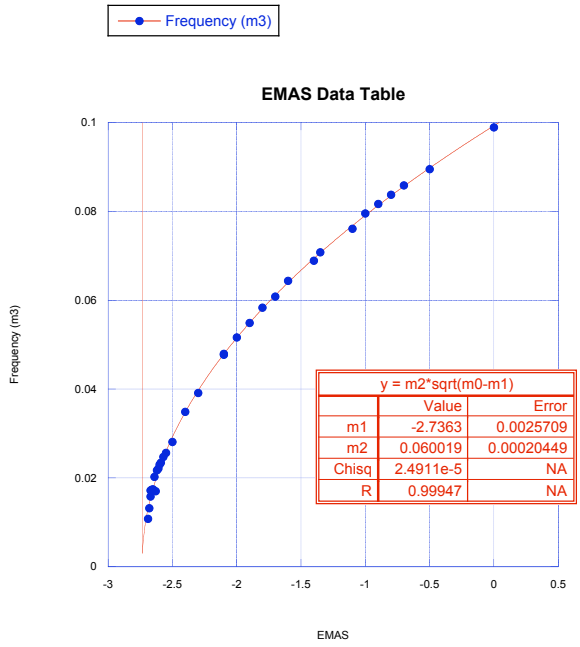

We give below a choice of fitting procedures to illustrate the process.
At EMAS = 0, the frequency is 0.0989 Hz with a statistical error of 10^{-6} and the lifetime is 495±2 s. As the EMAS is lowered, both frequency and the lifetime drop, which result in the Q factor decreasing as well (as Q is frequency*lifetime*pi).

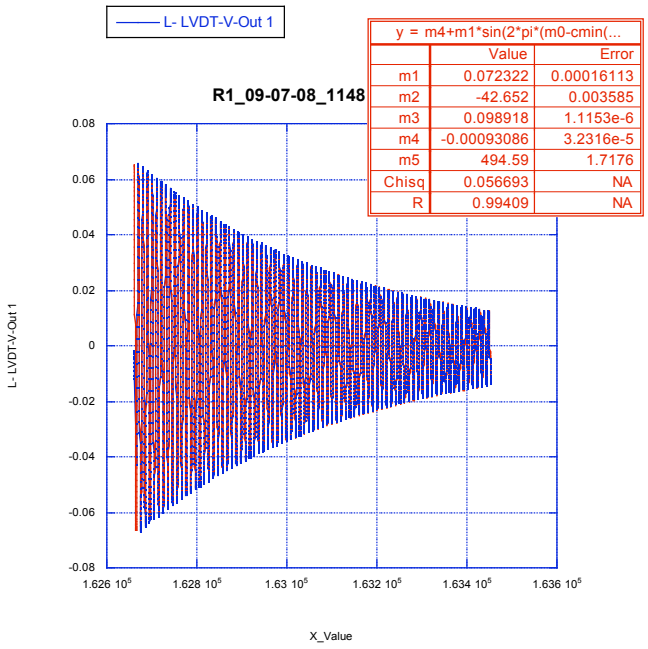

Next, for EMAS = -0.5, the frequency is 0.0895 Hz and the lifetime is 169 s. The fit is still good.

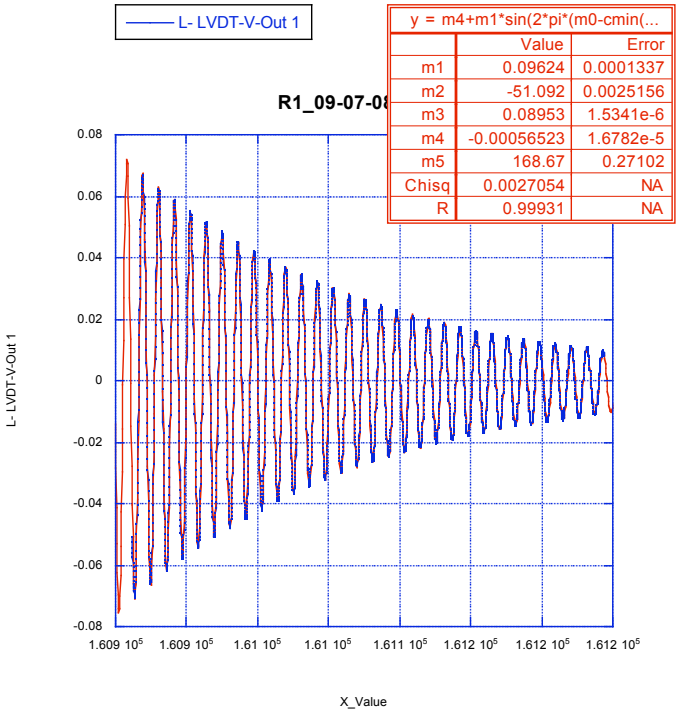

Next, for EMAS = -1.0, the frequency is 0.0796 Hz and the lifetime 105 s. Both values are progressively decreasing and the fit is still good.

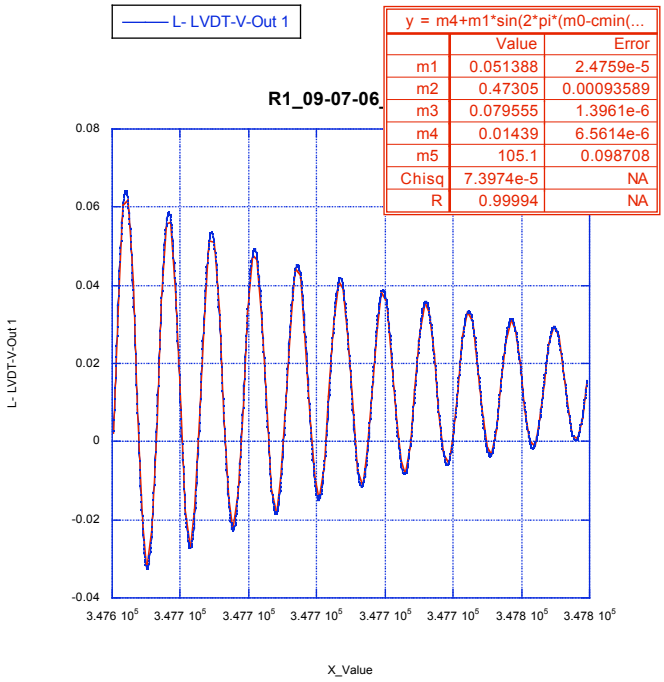

For EMAS = -1.7, the frequency is 0.0608 Hz and the lifetime is 69 s. The oscillations are dampening much more rapidly.

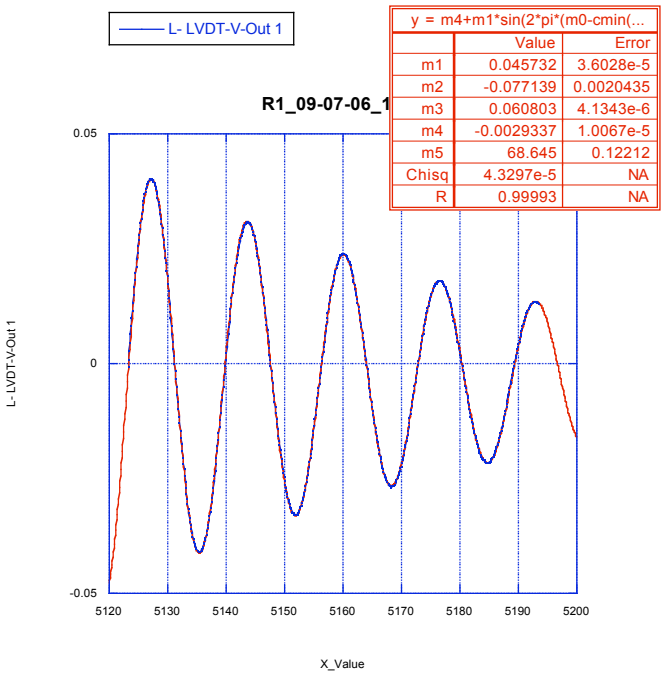

EMAS = -2.3; frequency is 0.0391 Hz and lifetime is 47 s.

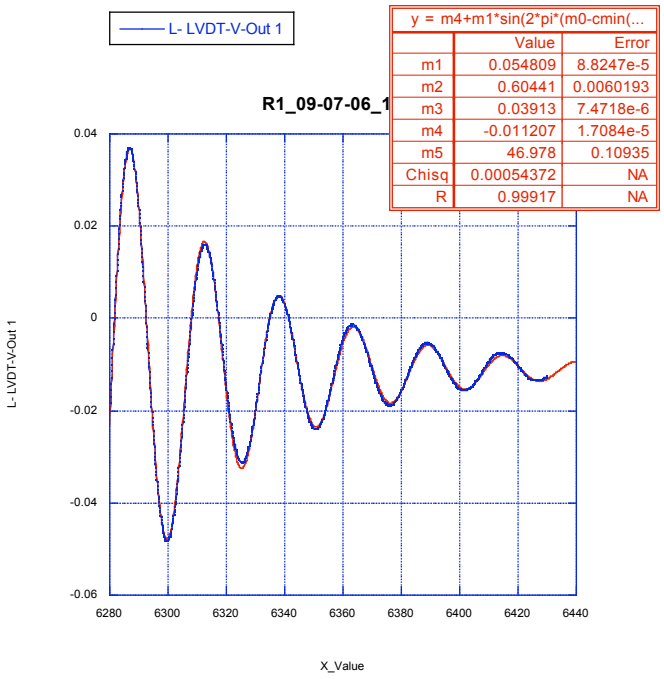

EMAS = -2.6; frequency is 0.0230 Hz and lifetime is 33 s. After only three or four oscillations, the system is already almost completely damped and enters the noise range.

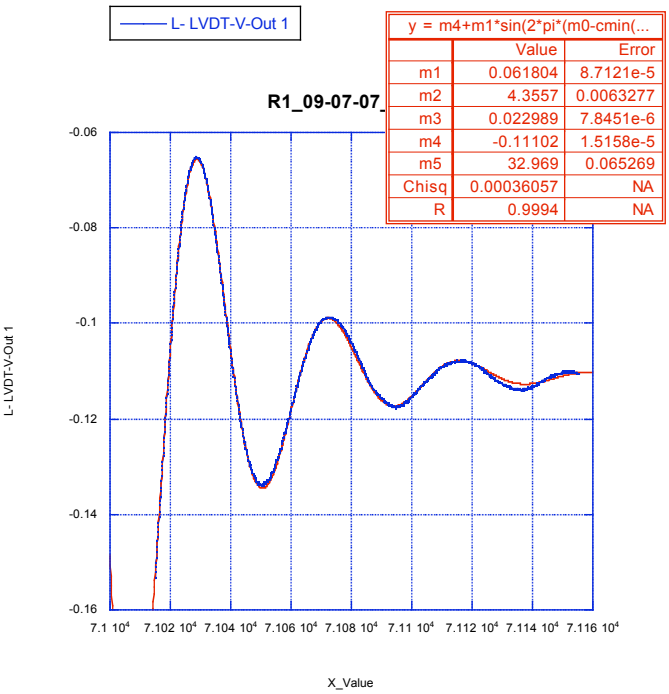

As the EMAS value approaches the system's falling-off point, we had to be very careful so as not to change the EMAS too significantly and disrupt the system. For EMAS = -2.63, the system underwent one oscillation before complete dampening. The frequency was 0.0170 Hz and the lifetime 40 s.

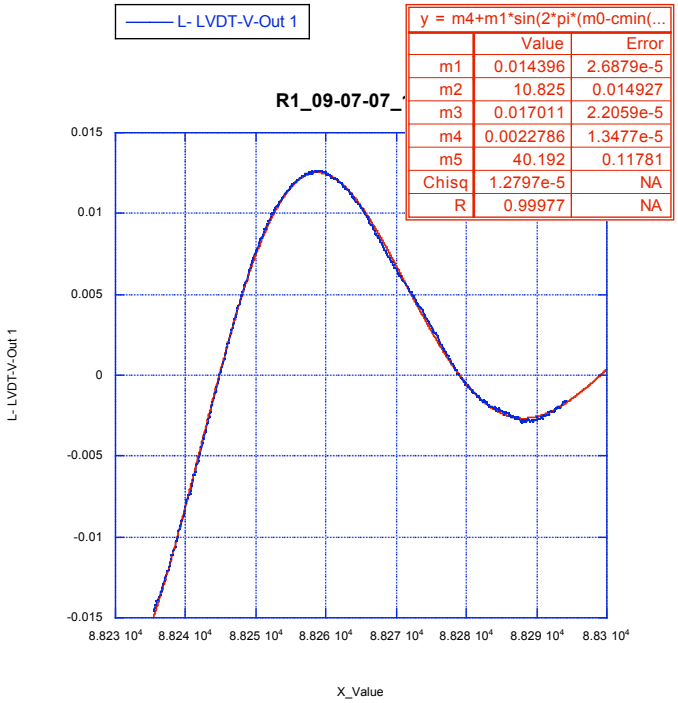

For EMAS = -2.67, the frequency was 0.0172 Hz and the lifetime 31 s.

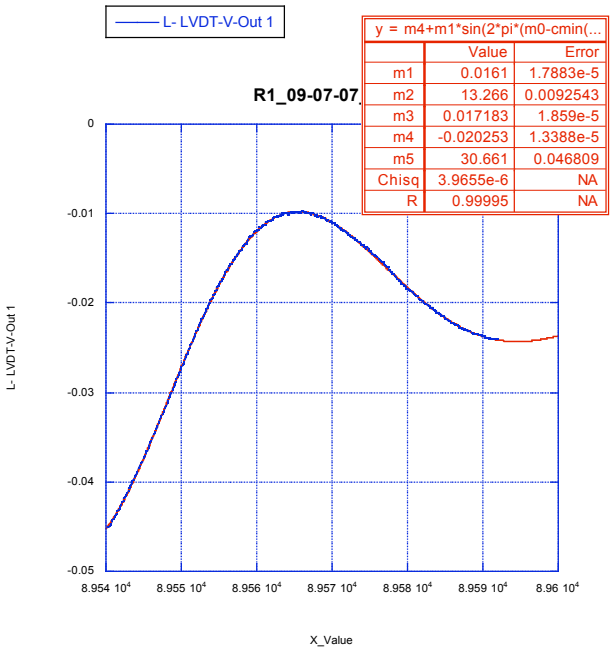

When the EMAS was -2.69, the system was still able to make one half-oscillation before drifting off course. The fitting starts losing meaning, however the fit values were frequency = 0.0108 Hz with a lifetime of 19 s.

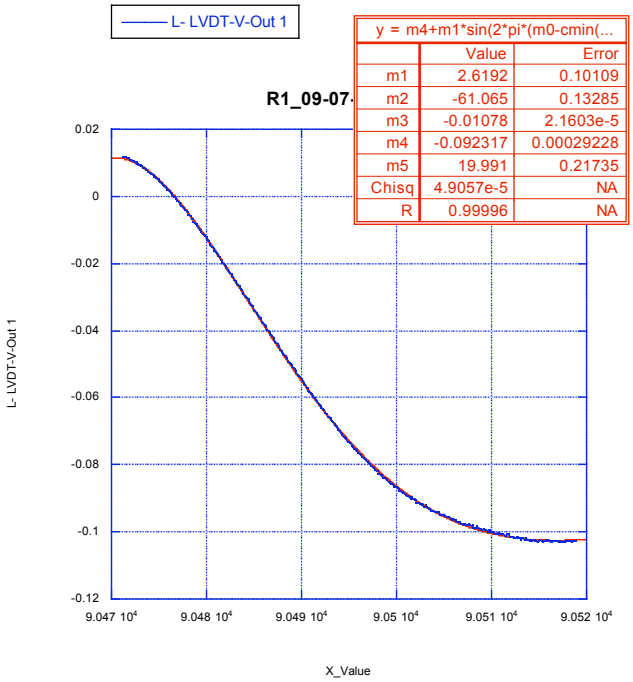

-2.69 curve fit: m4+m1*sin(2*pi*(m0-cmin(c0)-m2)*m3)*exp(-(m0-cmin(c0)-m2)/m5); m1=2.6192; m2=-61; m3=-0.01; m4=-0.092; m5=19.99.

The system became completely unstable at EMAS = -2.70. The system simply fell right away without oscillations then it started banging between the two end-stops.

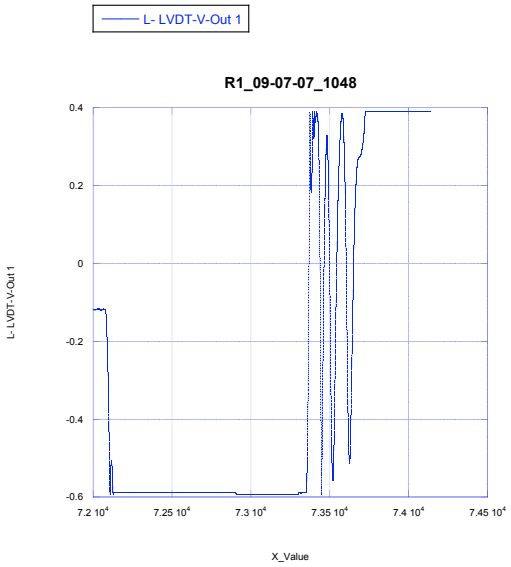

The frequency versus quality factor graph, when fitted to a curve, shows that at lower frequencies the data follows a quadratic trend, while at higher ones (from 0.07 Hertz and above) it follows an exponential curve.

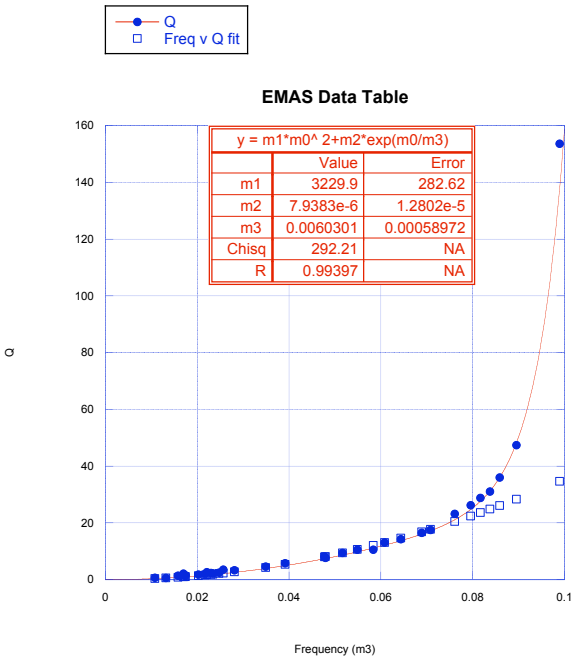

Curve Fit: m1*m0^ 2+m2*exp(m0/m3); m1=3229.9; m2=7.9e-6; m3=0.006;

To cross check that the EMAS feedback worked correctly, we repeated the procedure after altering the tuning mass load.
The additional data was compiled into the final summary graphs below. As expected, the EMAS versus frequency graph showed a continuous shift to the right with more and more mass removed from below the pivot point.
The trouble was in the frequency versus Q factor graph. Because gravitational restoring forces and EMAS are nominally equivalent, if the EMAS had worked perfectly the four curves should have overlapped perfectly. Instead the graph showed that for lower frequency values, the Q factor overlapped nicely, no matter the mass arrangement used for the trials. For lower gravitational restoring force (less mass below the pivot) and correspondingly less EMAS, the Q factor was higher, and the system dampens less.

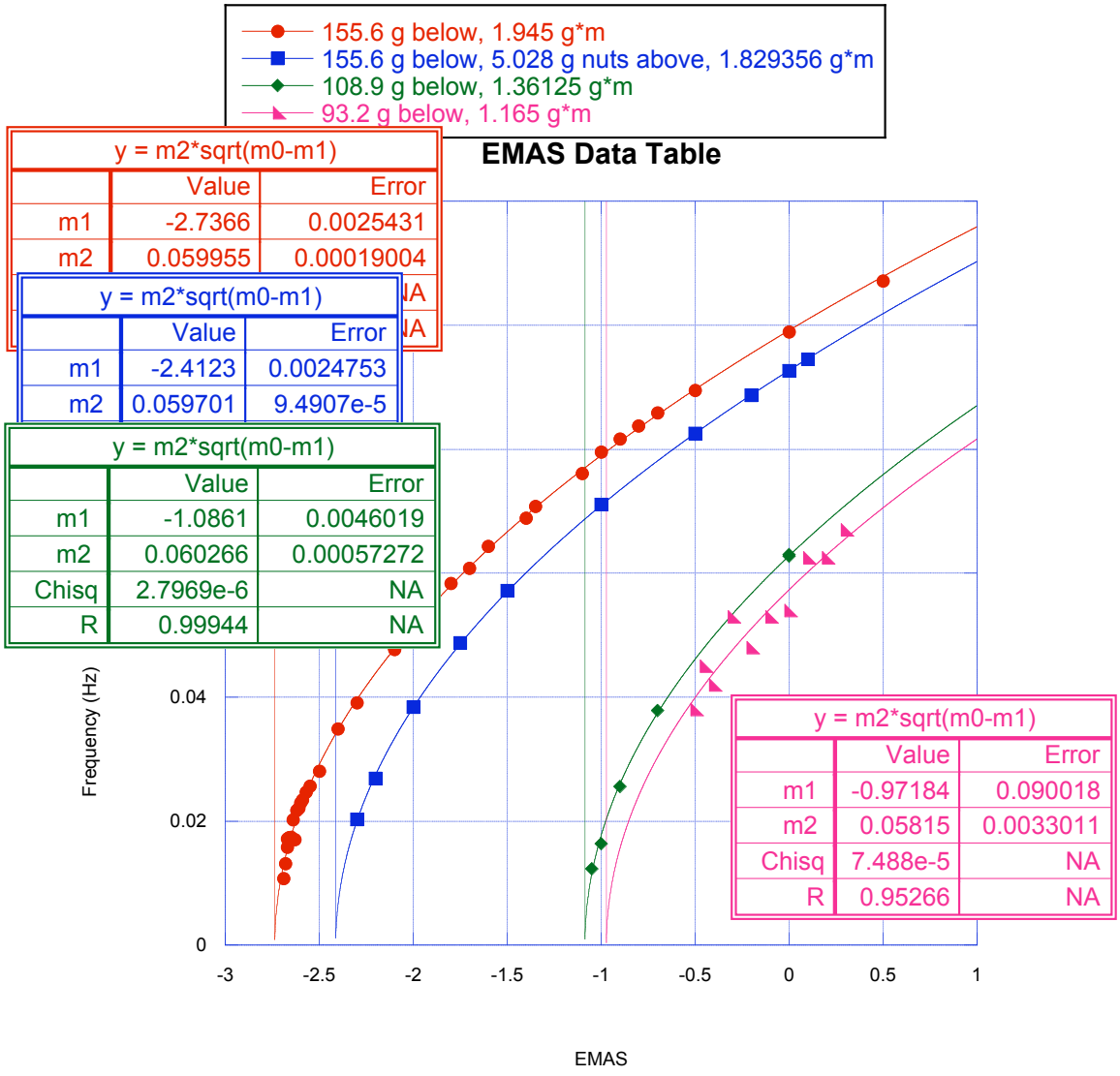

The mass configurations for each square root slope are as follows:
-2.7 EMAS endpoint: 4x 39 grams on the balance arm 12.5 mm below the pivot point
-2.4 EMAS endpoint: same as for -2.7 with 5.028 g of nuts placed on top of the arm (22.5 mm above the pivot)
-1.1 EMAS endpoint: 4x 27.225 g below the pivot point
-1.0 EMAS endpoint: 4x 23.4 g below the pivot point.

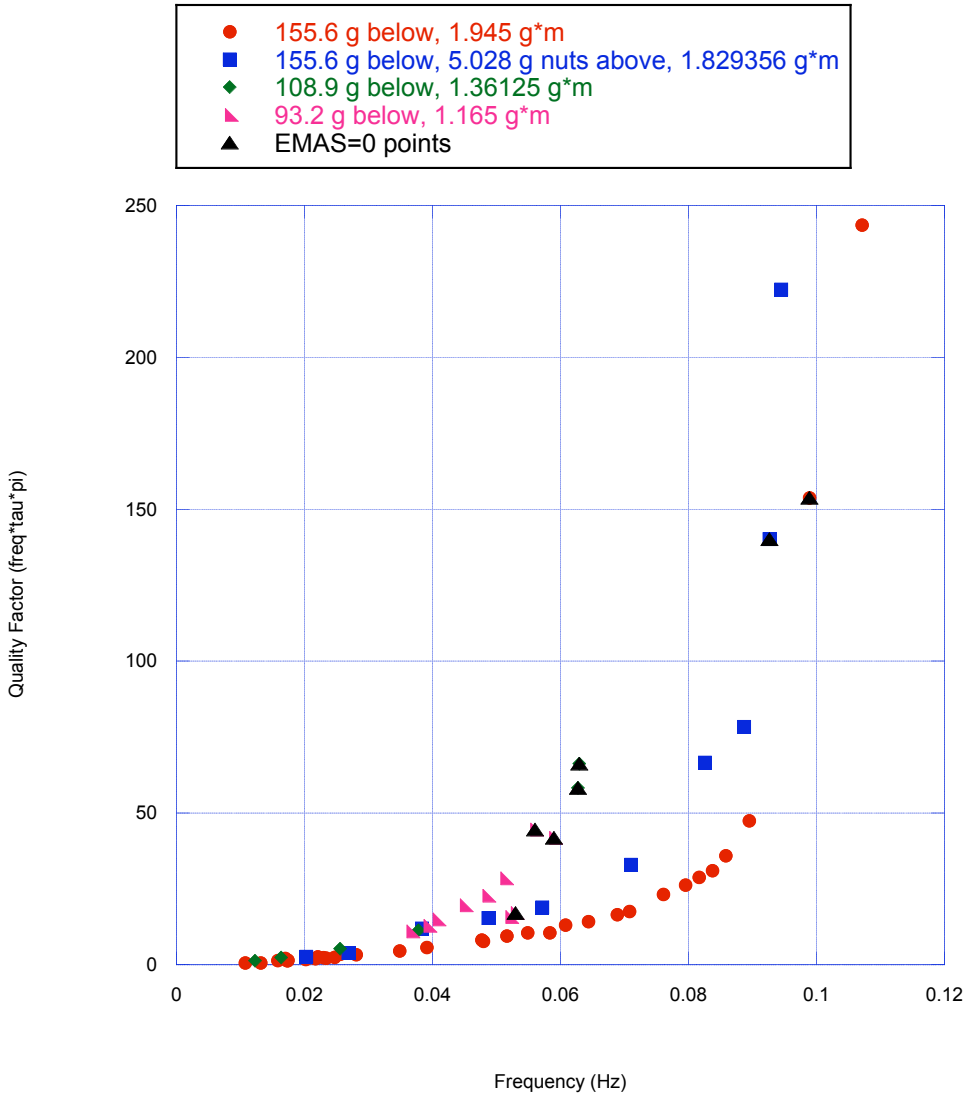

We had expected the quality factor vs. frequency graphs to overlap, independent of the EMAS used. The fact that this did not occur shows that there was a problem with the EMAS section of the program, falsifying the quality factor measurements. The black triangular points on the graph above are where EMAS is equal to zero for each mass configuration and therefore are the only true measurements of the tiltmeter quality factors that can be retained. The frequency vs. EMAS measurements remain valid and can be retained.

For the first set of EMAS data, the masses on the tiltmeter totaled 155.6 grams at 12.5 mm below the pivot point. The second set of data had the same masses below, and 5.028 grams in nuts at 23 mm above the pivot point. For the third set of data (the third square root slope from the left on the graph), we removed the nuts on top and some of the mass below, making a total of 108.9 grams at 12.5 mm below the pivot point. The fourth and final set of data had 93.2 grams at 12.5 g below the pivot point. The total torque of the system for each respective set of data was 1.945 g*m, 1.829 g*m, 1.361 g*m, and 1.165 g*m.

2.3 Positive values of EMAS

I took one data test for an EMAS value above zero (0.5). When I tried graphing the data using the same sine and exponential curve, I could not do so because the system was ringing up over time instead of the intended ringdown effect.

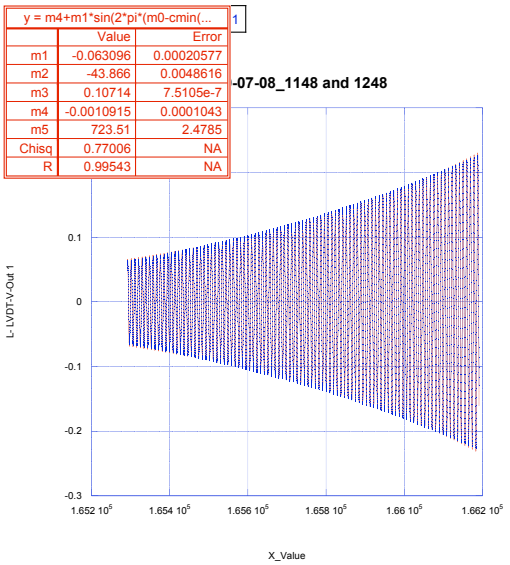

m4+m1*sin(2*pi*(m0-cmin(c0)-m2)*m3)*exp((m0-cmin(c0)-m2)/m5); m1=-0.0632; m2=-43; m3=0.107; m4=-0.001; m5=723;

This is an indication that something is wrong in the system, be it mechanical or electrical (electrical perhaps being that the computer was sending some undetected and unwanted feedback into the system that continuously gave energy to the system and re-excited it. The most likely culprit is the possibly too slow feedback loop speed, which was only 10 Hz in this initial round of tests.

To change the resonant frequency of the system we put three evenly placed nuts of mass 0.838 g on each end of the tiltmeter (a total mass addition of 5.028 g). This is a 0.023 m above the pivot point. Being above the pivot point it makes an inverted pendulum of $K_{a\text{-}gray\_nuts} = mgl$: more mass is more destabilization and higher is also more destabilization.

For the curve fits of the kicks to the system with changing EMAS, we found that both the frequency of oscillation and the lifetime changed with time. As the amplitude decreased, the frequency and lifetime, and thus quality factor, both increased. Since the ultimate goal of the tiltmeter is to measure very low seismic motion with very low amplitudes of movement, we want to pay attention to the smaller motions of the system.

3 Hysteresis Testing

Beginning on August 3, we began testing the tiltmeter using a new program that sent out a sinusoidal signal which slowly moved the tiltmeter to a specified amplitude, flattened out, then slowly brought the tiltmeter back to zero with very little oscillation. In measuring the mean of the data points before, during, and after the slow step, we can determine the hysteresis of the tiltmeter.

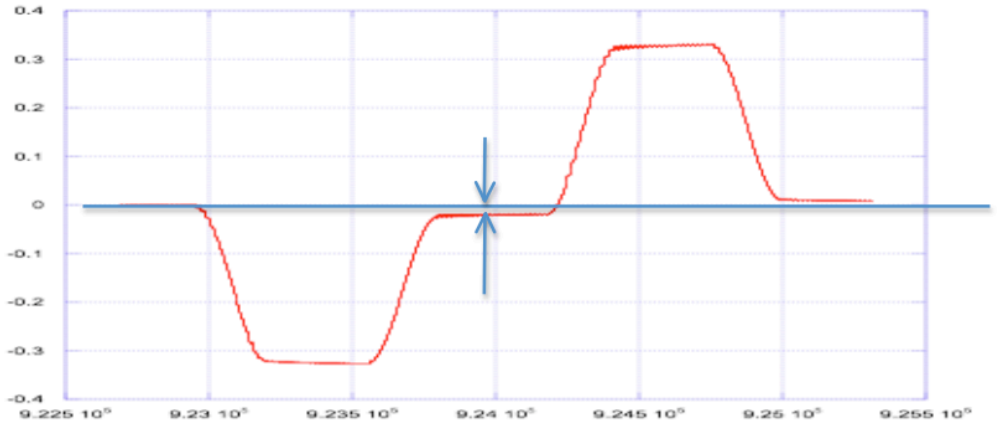

The movement of the tiltmeter and the hysteresis measured after each slow step

For each EMAS, we sent out the sinusoidal signal at a fraction ($1/30^{th}$) of the natural frequency of the system (to determine this we referenced the square-root graph already determined by our measurements of the ringdowns of the kicks to the system). Because hysteresis in any system is a memory of the past positions, we repeated each step at a certain amplitude 3 or 4 times in succession. Averaging the positions of the small oscillations of the LVDT immediately before the step up, immediately before the step down (at the largest amplitude), and about 5 minutes after the system calms down, we were able to determine both the actual amplitude the system moved for each EMAS and the hysteresis of the system, given by the difference between the position before and after each full step.

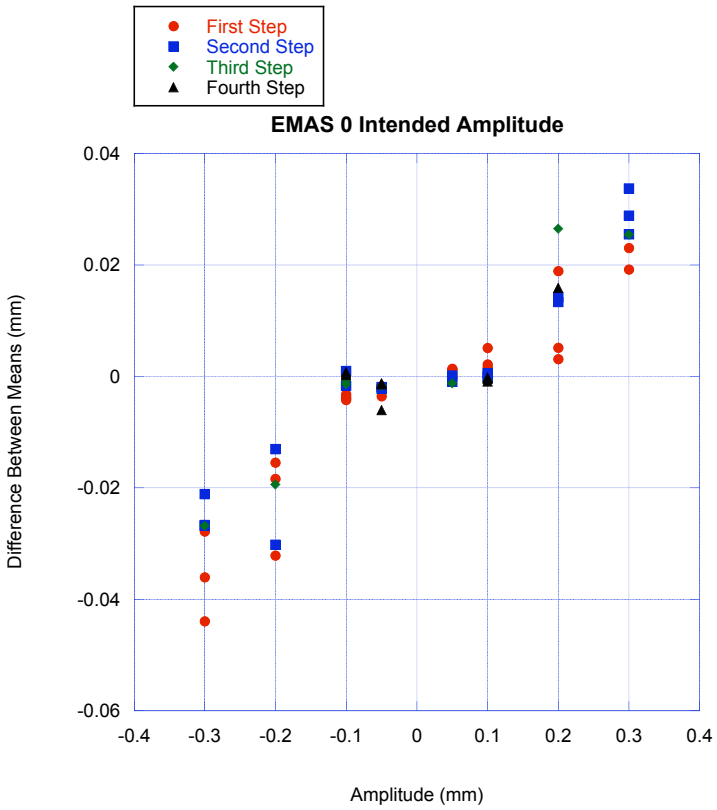

EMAS = 0, control input amplitude in mm versus hysteresis in mm

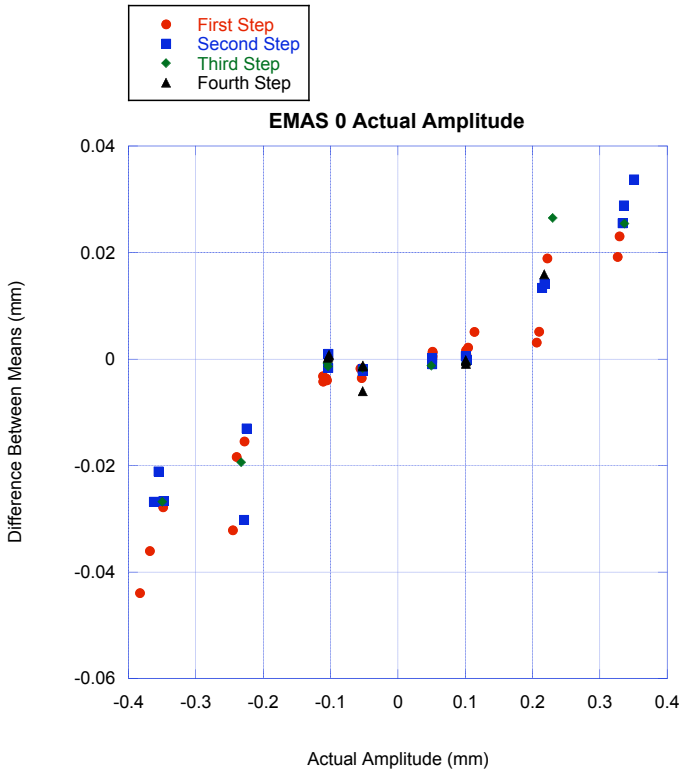

EMAS = 0, resulting amplitude in mm versus hysteresis measurement in mm

We expected the data to show that the hysteresis had a linear dependency on the amplitude of the step. However, both graphs show that for amplitudes closer to zero, the slope of hysteresis leveled out to almost zero. A possible explanation for this is that the knife-edge is cut in a way so that the tip is slightly blunted and thus results in less hysteresis if only moved a little bit. Testing the system again with a sharper knife-edge or a flexure blade would hopefully cancel out this problem and yield better results. If that is not the case, this small slope shows that the system is good, for its purpose is to test for motion at very low, seismic amplitudes. Having zero hysteresis for zero step amplitude is the intended result.

I took data for three other EMAS values, and some of the graphs showed the same leveling out at zero amplitude. Below, the EMAS = -0.1 graphs show a small leveling out, but one not as clearly defined as in EMAS = 0.

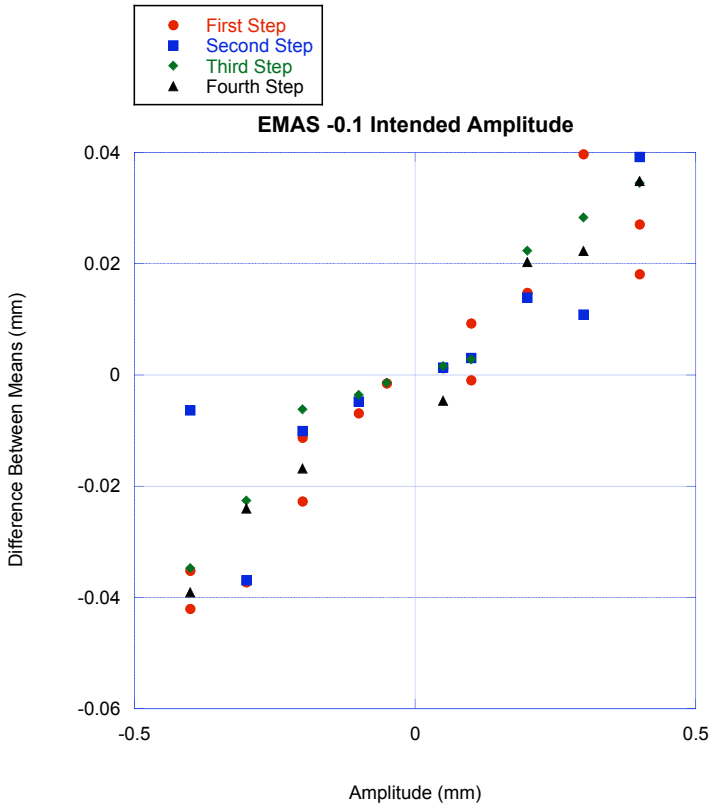

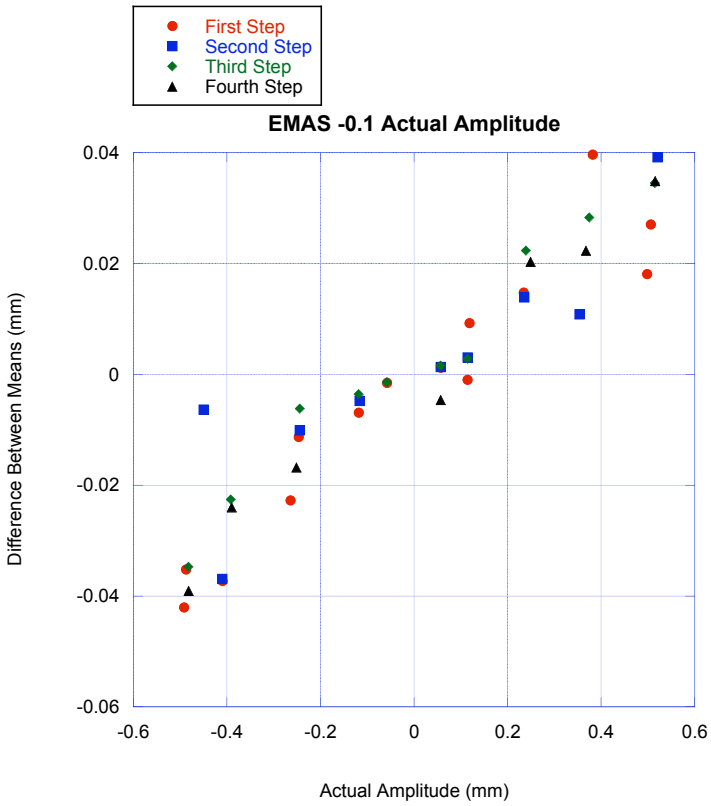

The EMAS = -0.2 graphs show some, but very little, leveling out near zero amplitude.

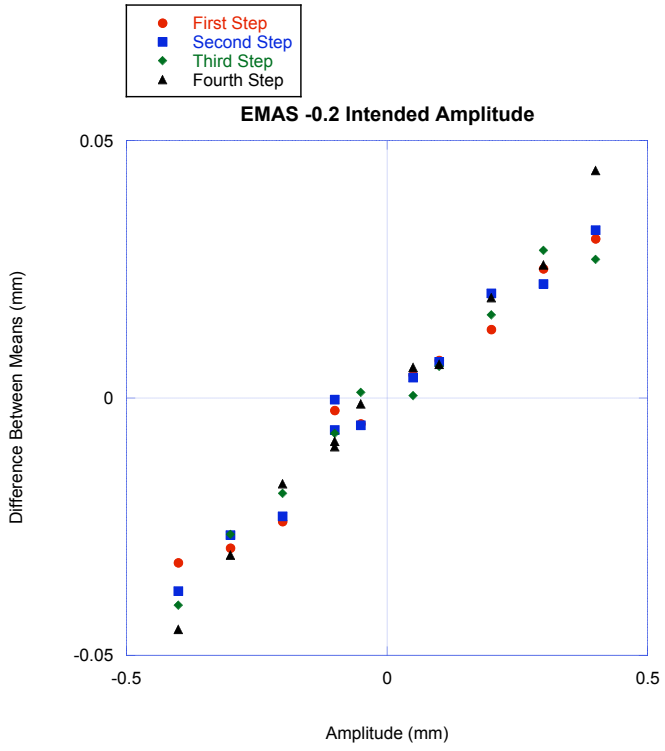

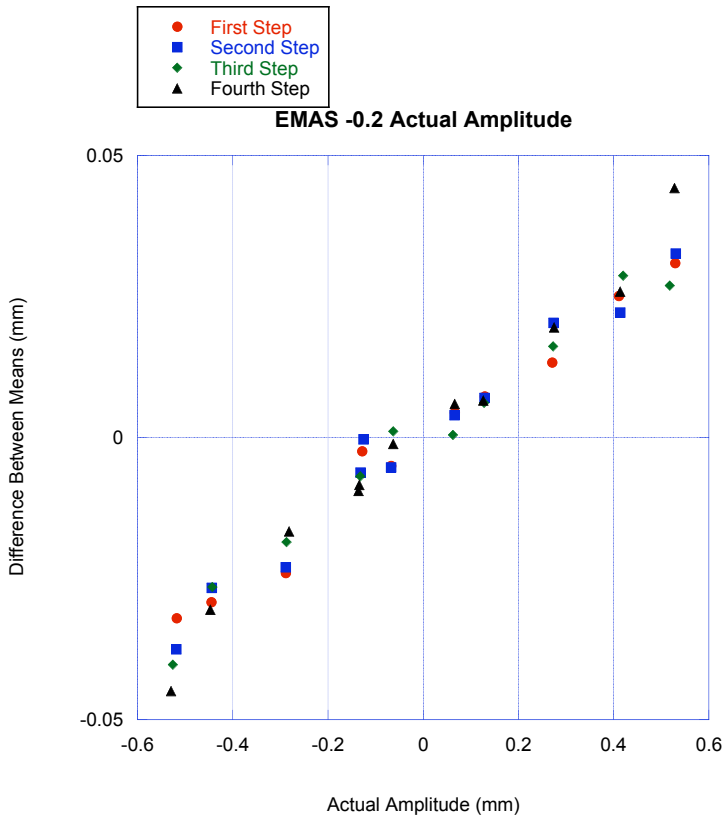
First Step
Second Step
Third Step
Fourth Step
EMAS -0.2 Actual Amplitude
0.05
0
-0.05
-0.6
-0.4
-0.2
0
0.2
0.4
0.6
Difference Between Means (mm)
Actual Amplitude (mm)

The EMAS = 0.3 graphs show clear leveling out again.

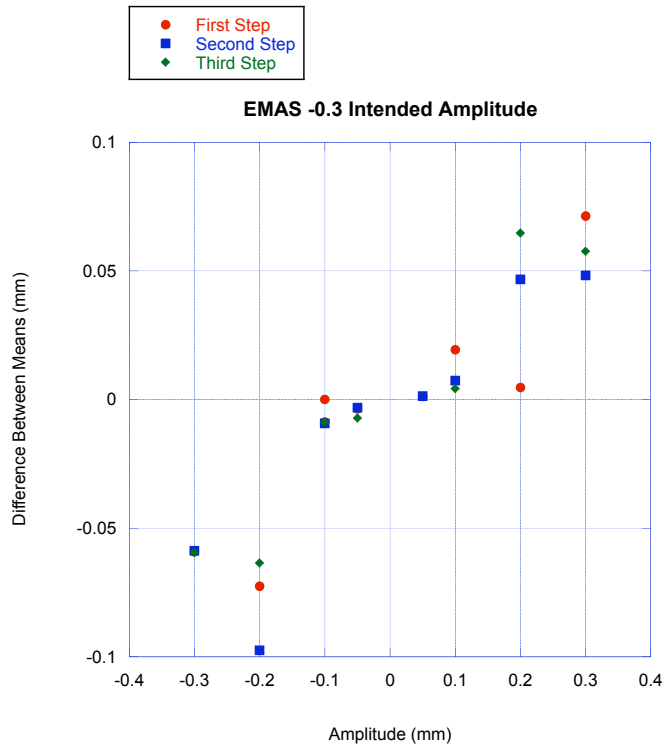

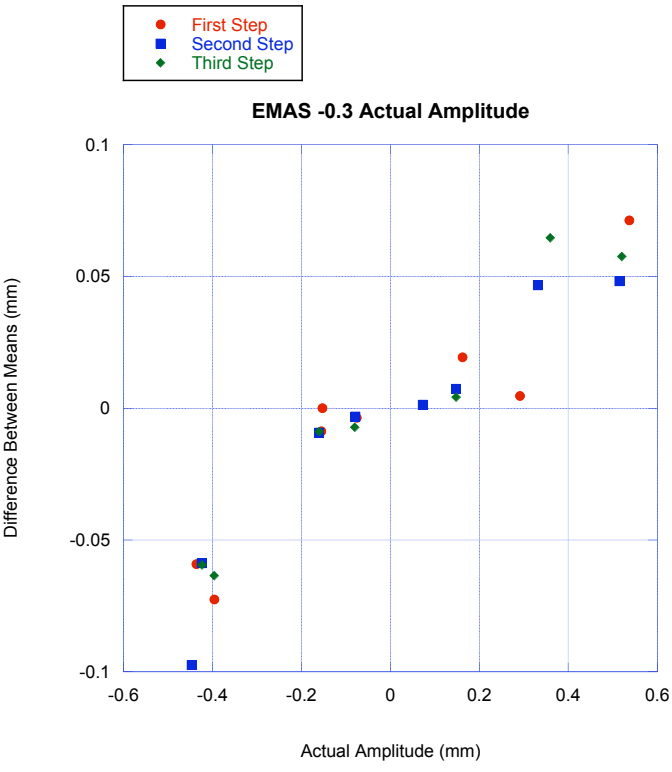

I performed a linear curve fit on the small amplitude data (between -0.1 and 0.1 mm) for each EMAS value to find the hysteresis.

EMAS = 0:
y = -0.00068613 + 0.013769x
With zero EMAS gain, the system has only about 1.4 percent hysteresis.

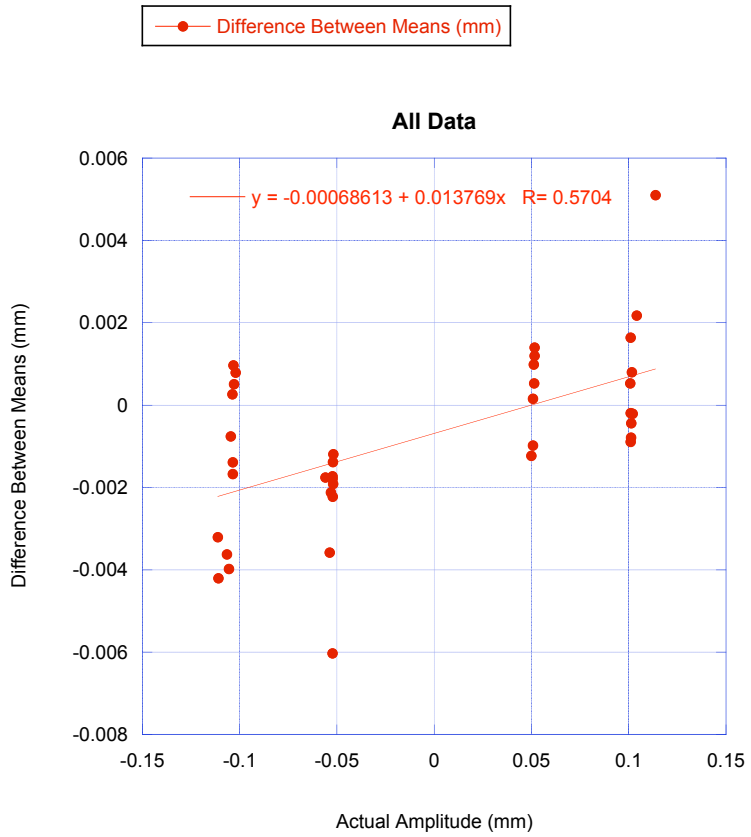

EMAS = -0.1:
y = -0.00092363 + 0.033178x
With -0.1 EMAS gain, the system has 3.3 percent hysteresis.

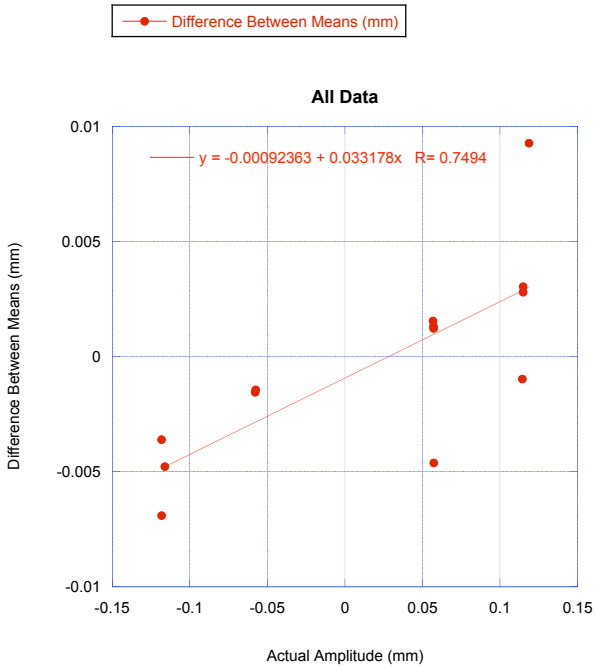

EMAS = -0.2:
y = 0.00062819 + 0.048266x
With -0.2 EMAS gain, the system has 4.8 percent hysteresis.

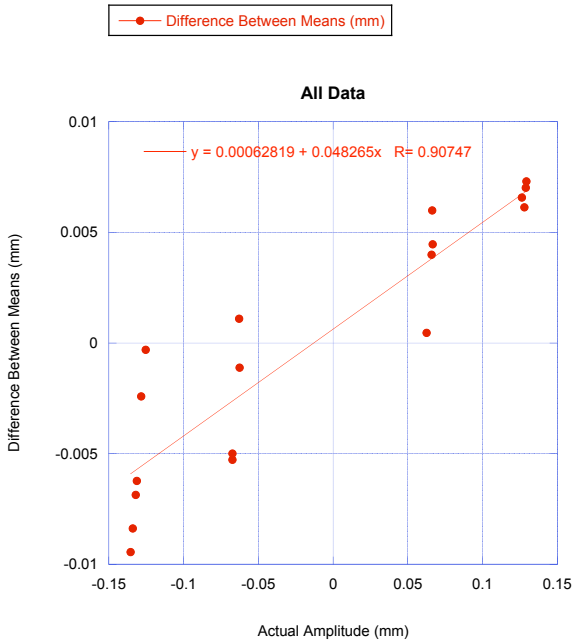

EMAS = -0.3:
y = 0.00056251 + 0.053166x
With -0.3 EMAS gain, the system has 5.3 percent hysteresis.

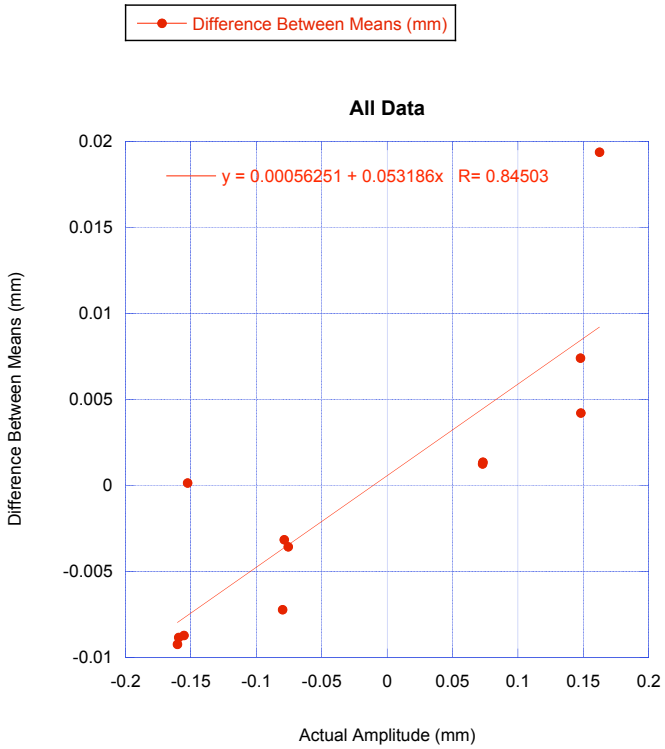

As the EMAS decreases, the hysteresis slope increases. The system is more and more unstable (less elasticity and lower quality factor) and thus does not return to the previous position as much after each step. Plotting this slope versus the EMAS gain yields this graph:

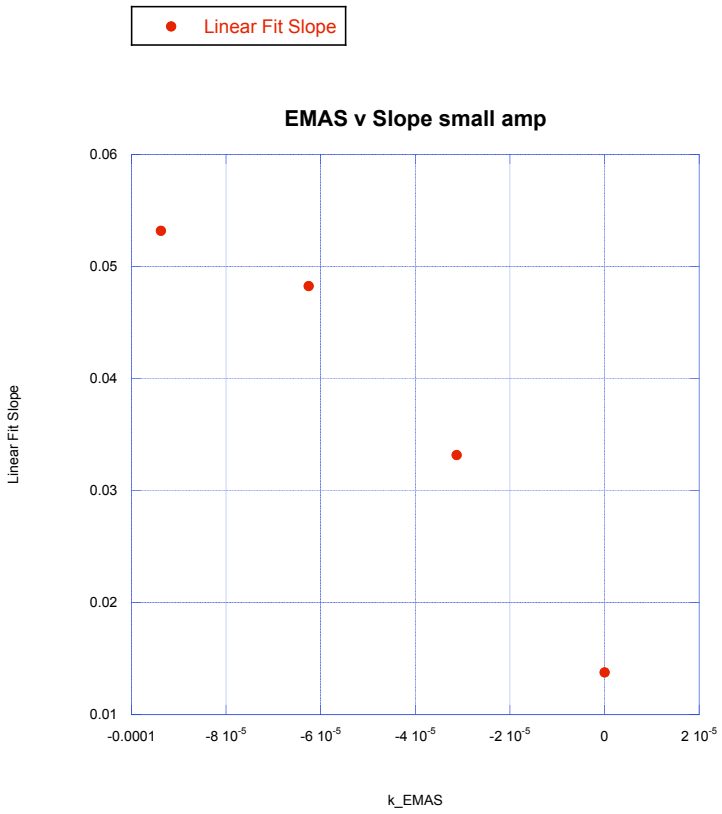

More testing, with a fixed EMAS program, a flexure or sharper and harder knife-edge (a new one will be made of tungsten carbide with titanium nitrite polish), and further data measurements with more EMAS gain values, can help determine if this relationship is linear or quadratic.

The same data above but without the first step data measurements (which have the most "memory" and thus the greatest hysteresis) yields the following graphs.

EMAS = 0:
y = -0.00087223 + 0.00078998x
With zero EMAS gain, neglecting the first step data, the system has 0.08 percent hysteresis.

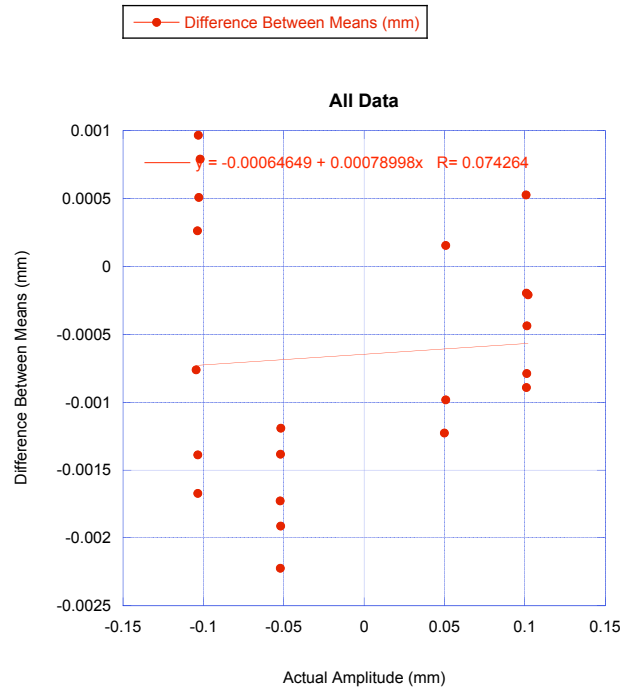

EMAS = -0.1:
y = -0.0010676 + 0.026131x
With EMAS gain -0.1 and neglecting first step data, the system has 2.6 percent hysteresis.

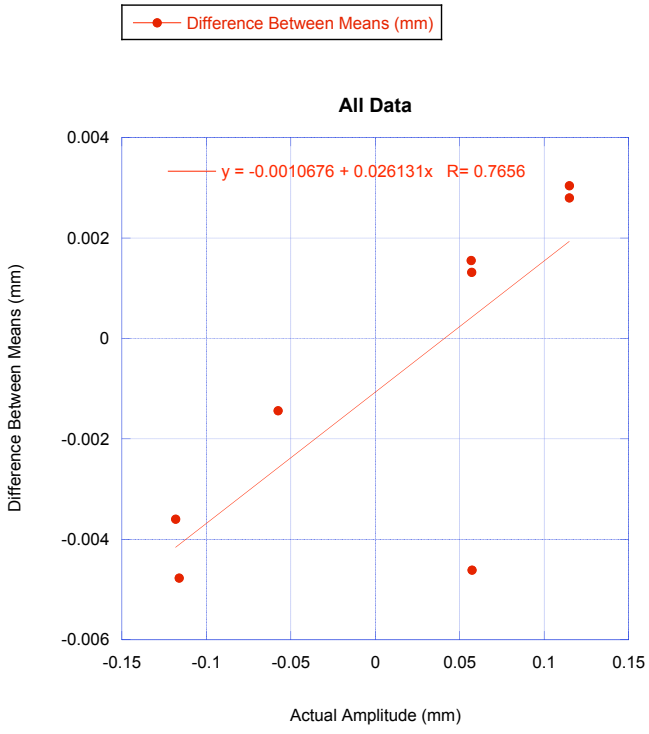

EMAS = -0.2:
y = 0.00050908 + 0.048981x
With EMAS gain -0.2 and neglecting first step data, the system has 4.9 percent hysteresis.

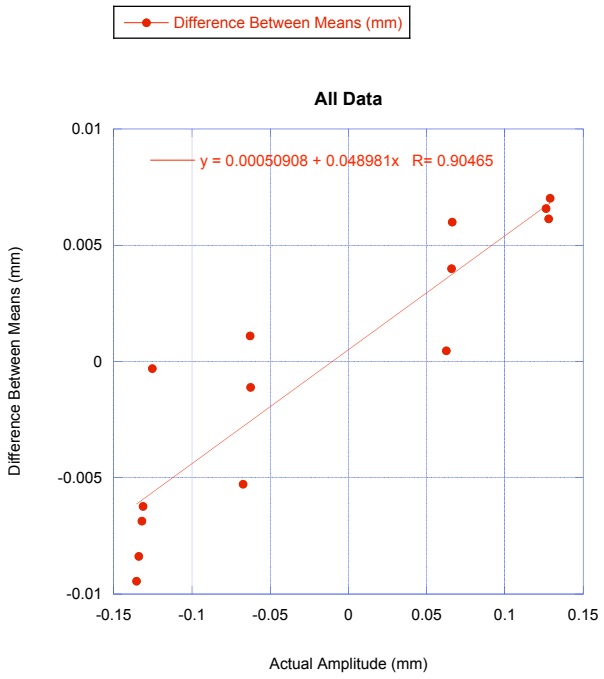

EMAS = -0.3:
y = -0.001464 + 0.047582x
With -0.3 EMAS gain and neglecting first step data, the system has 4.8 percent hysteresis.

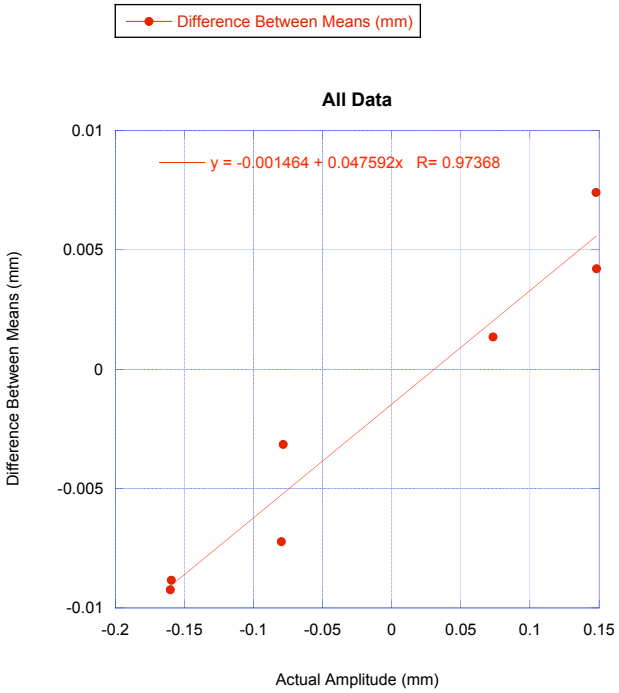

The same EMAS vs. slope graph above, but ignoring the first step data, becomes:

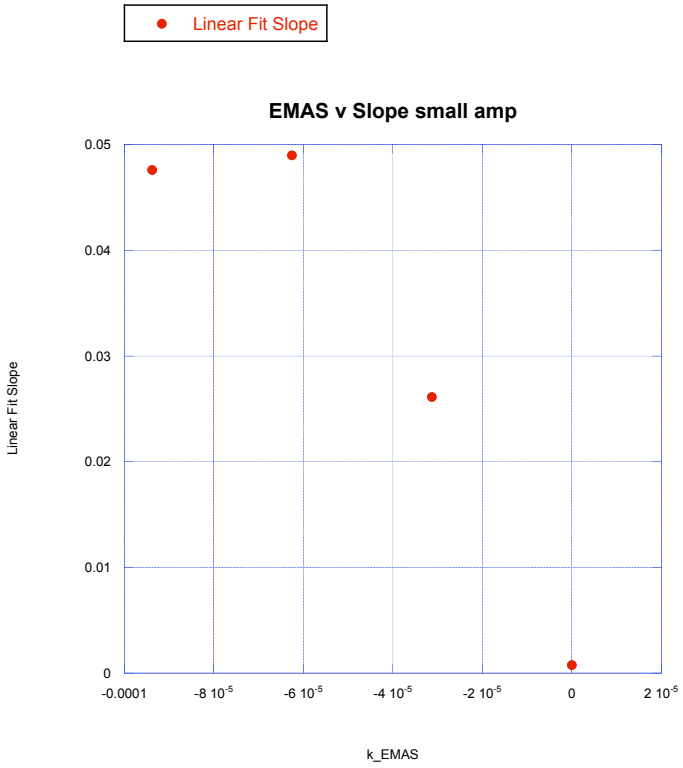

The same decreasing relationship is seen, but the possible quadratic curve is not as clearly defined, and the possible linear curve even much less so.

The tiltmeter is intended to be in use at zero EMAS gain. The best data shows that the hysteresis using this parameter is only about 0.08 percent. This value could possibly be lowered significantly or removed completely if the drift over time is taken into account. We were unable to measure the hysteresis of the system at lower amplitudes than 0.05 because of this drift. Measurements taken over an hour or two, leaving the system quiet, show this drift.

3.1 Drift Measurements

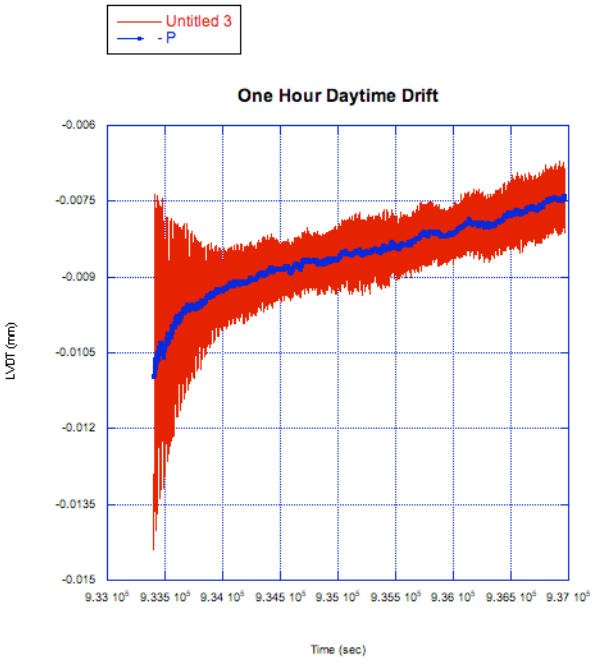

According to this drift data, the system moves 0.0000597 mm per minute of rest. If the system is at rest for 5 minutes between each step, this amounts to 0.0003 mm of drift, lowering the hysteresis even more, to 0.05 percent.

Looking at another set of drift data, in which the system drifts toward the negative LVDT direction, we see that it moves -0.000134 mm per minute, and -0.000668 mm per 5 minutes, and -0.00802 mm per hour.

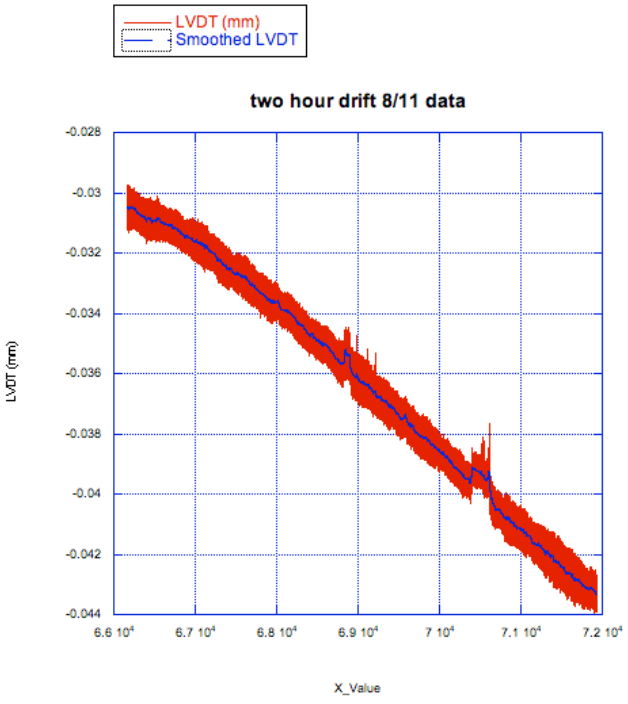

4 Step Function Analysis

We began to take data with different EMAS values, probing the system with a sudden force step function then returning to zero to look for hysteresis. However, because the steps jump to and from zero, they oscillate and most likely erase hysteresis. After each step, up or down, we let the system stabilize for approximately twenty minutes to reach its equilibrium and measured the static level by taking a portion of data and finding the average. We did this to see if the system would return to the same level after the step as it had been prior to the step. If not, we look for a trend in the difference from beginning to end. Following the observation that positive EMAS values ring up the system, we only took tests with negative EMAS values.

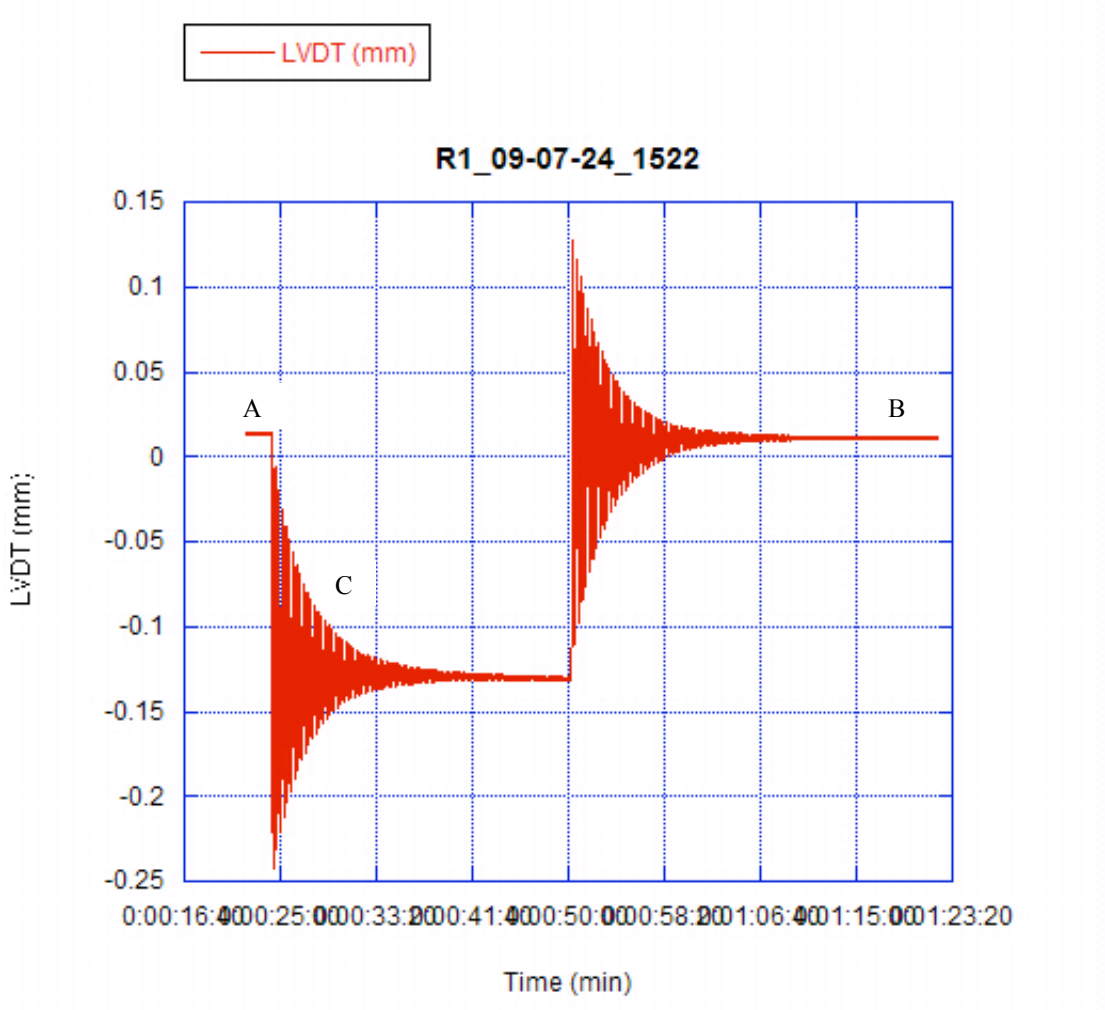

Plot of 0.1 step amplitude at -0.1 EMAS.

With this graph, as well as others like it, we compared level ***A*** with level ***B*** to see any change. We also documented the amplitude of the oscillations at level ***C***.

After each step-cycle, we noticed that the ending LVDT amplitude was slightly smaller than the beginning value. This could be happening as a result of expected hysteretic energy loss. The change was negative for all positive steps but when we tried a negative step, the change in the level before the step to after was positive.

EMAS	Start LVDT	Step Kick	End LVDT	Change: 0 to 0
0	0.009	0.1	0.0045	fell by 0.0045
-0.1	0.014	0.1	0.011	fell by 0.003
-0.2	0.012	0.1	0.0095	fell by 0.0025
-0.3	0.01	0.1	0.0085	fell by 0.0015
-0.4	0.01	0.1	-0.065	fell a lot: by 0.075
0	0.001	-0.5	0.0015	rose by .0005

Table of values, specifically the change in the equilibrium point from beginning to end of the step function.

At EMAS -0.2, we found the difference between the LVDT amplitude at ***A*** and ***B***.

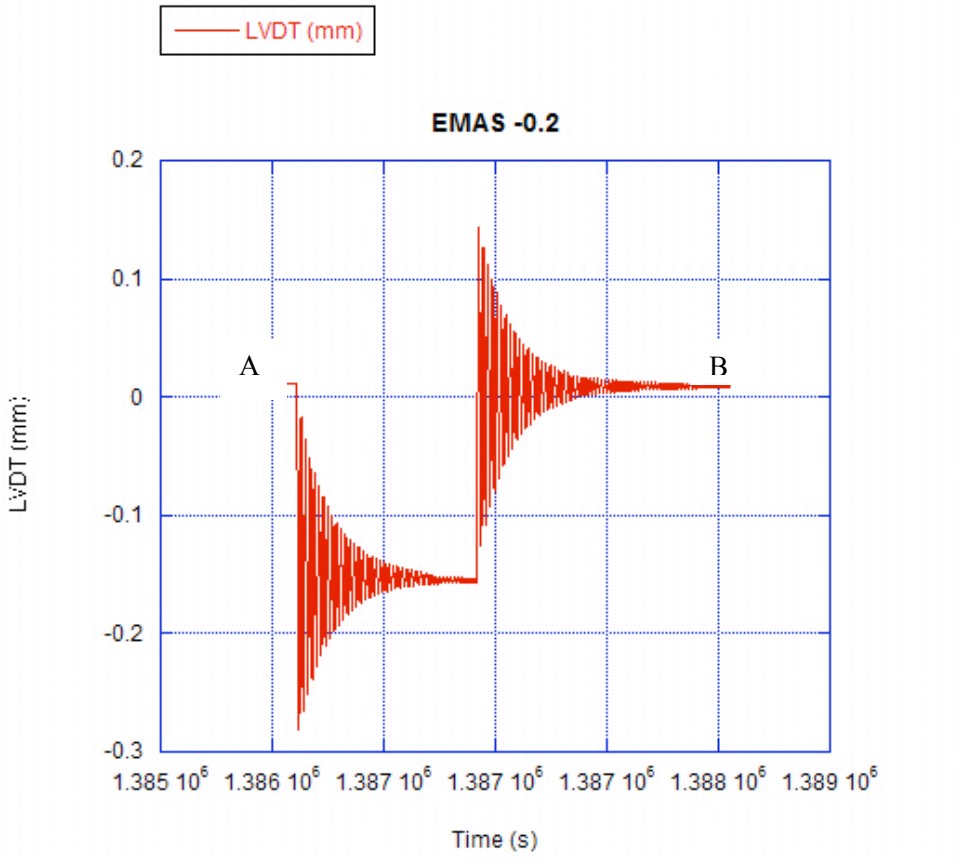

The graph of EMAS -0.2 with 0.1 step amplitude.

By looking at the graphs of the data, we were able to find the frequency and lifetime and then we multiplied both by pi to find the Q Factor:

EMAS	Start LVDT	Step Amp	Step LVDT	Frequency of Step	End LVDT	Change: Step to 0	Lifetime	Q Factor	Stiffness (k)
0	0.009	0.1	-0.117	0.056	0.0045	rose by 0.122	245	43	0.00345744
-0.1	0.014	0.1	-0.13	0.056	0.011	rose by 0.141	165	29	0.00390625
-0.2	0.012	0.1	-0.155	0.053	0.0095	rose by 0.165	259	43	0.00226576
-0.3	0.01	0.1	-0.19	0.048	0.0085	rose by 0.199	122	18.4	0.00207025
-0.4	0.01	0.1	-0.369	0.042	-0.065	rose by 0.304	108	14.3	0.00173889

A table of values based on different EMAS tests.

Stiffness

	EMAS	Freq...cillation	Q-factor	step	step up	step ...to down	hyste...s (mm)	Fract...teresis	Stiffness
0	0.0000	0.056000	43.000	0.10000	-0.11700	0.12200	0.0045000	0.036885	0.0034570
1	-0.10000	0.056000	29.000	0.10000	-0.13000	0.14100	0.0030000	0.021277	0.0039060
2	-0.20000	0.053000	43.000	0.10000	-0.15500	0.16500	0.0025000	0.015152	0.0022660
3	-0.30000	0.048000	18.400	0.10000	-0.19000	0.19900	0.0015000	0.0075377	0.0020700
4	-0.40000	0.042000	14.300	0.10000	-0.36900	0.30400	0.075000	0.24671	0.0017390
5									

A KaleidaGraph table of similar values.

We then plotted the stiffness of the spring versus the change from step to zero:

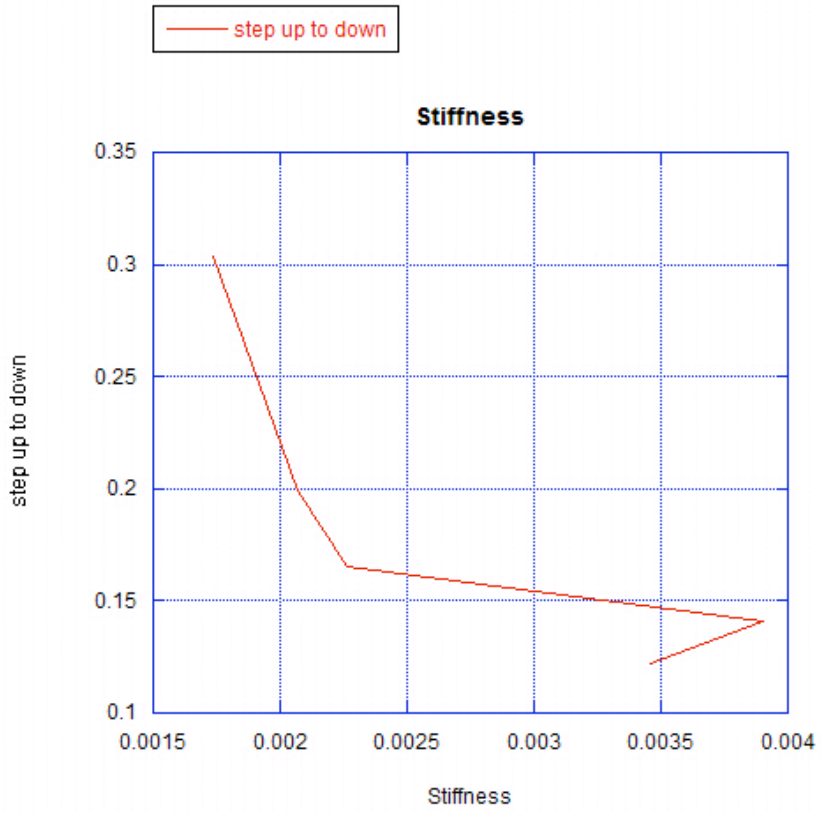

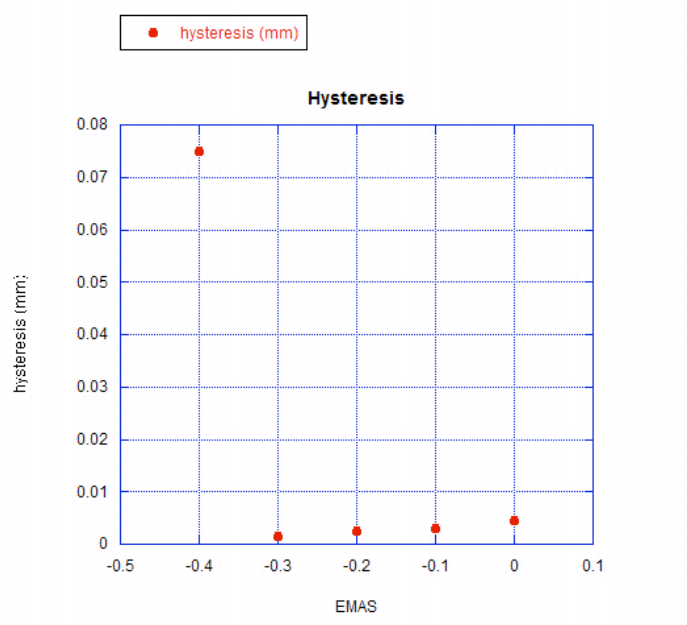

EMAS values versus observed hysteresis.

The graph of EMAS versus hysteresis is interesting because there is less hysteresis at lower EMAS values. It was expected that at a softer system we would be able to see more hysteretic movement.

5 System Noise Analysis (Part I)

We took data over the 4th of July weekend (from the evening of the 3rd to the morning of the 6th) with all feedbacks off (zero EMAS and the position integrator on pause), to test the mechanical stability of the tiltmeter and the stability of the acquisition program.
The acquisition included the following channels:
1) Integrator
2) Current Request
3) LVDT, displacement of the tiltmeter arm measured in mm (conversion internal to the program)
4) Output of Coil 1
5) Input of Coil 1
6) Output of Coil 2
7) Input of Coil 2

The data was divided in four parts for convenience and the LVDT signals were inspected first. In the first quarter we found four jumps and two small physical excitations (the tiltmeter is excited and oscillates and rings down regularly).
The jumps are unphysical, must be software or DAQ card related, as they do not involve ringdowns).
In the second quarter we observe a single, prolonged, jump. The third quarter is quiet and well behaved, and the last quarter is quiet, except for two large re-excitations, possibly related with activities in and near the lab as activities are resumed after the vacation.

5.1 LVDT

First quarter of the data **Time=0** corresponds to **11:16 AM** on **July 2** when we started acquiring the data:

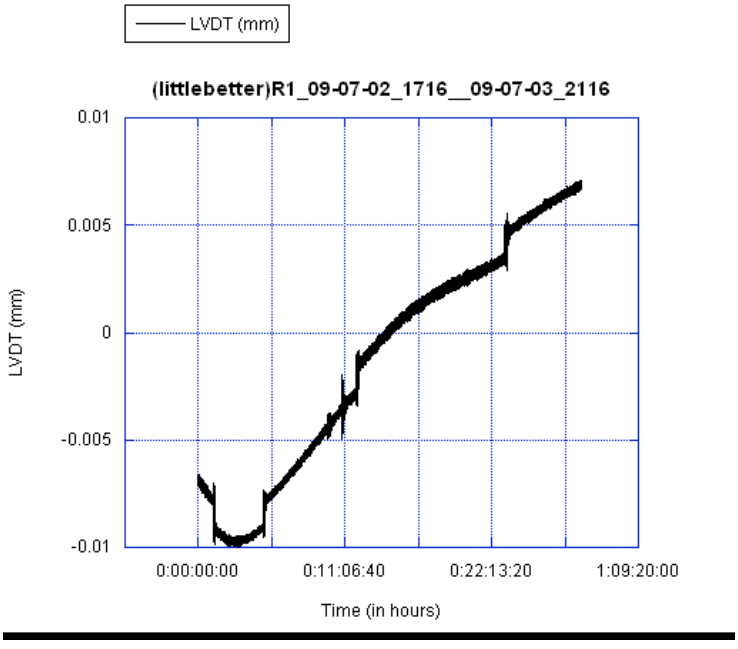

Second Quarter of the Data:

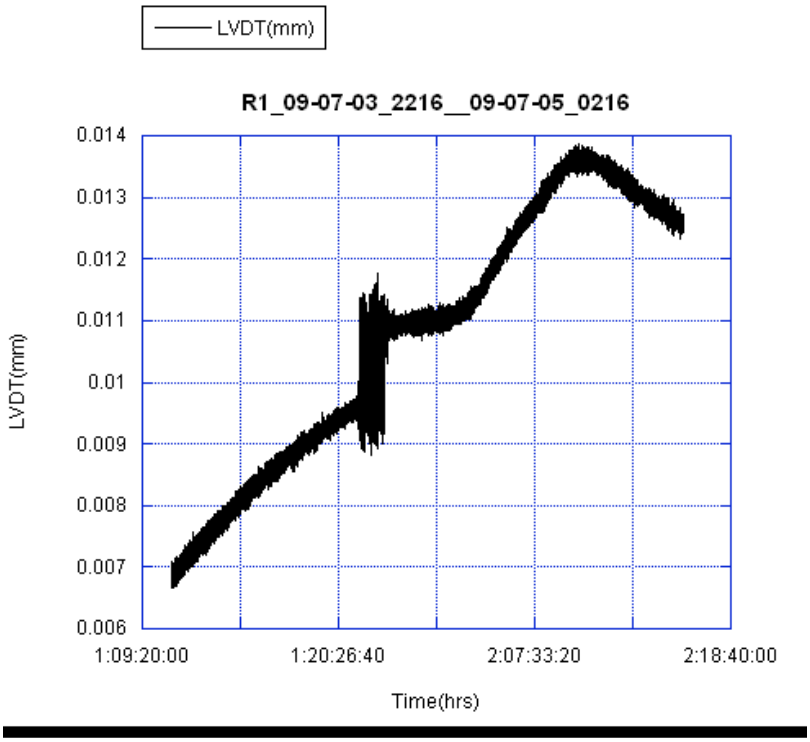

Third Quarter of the Data:

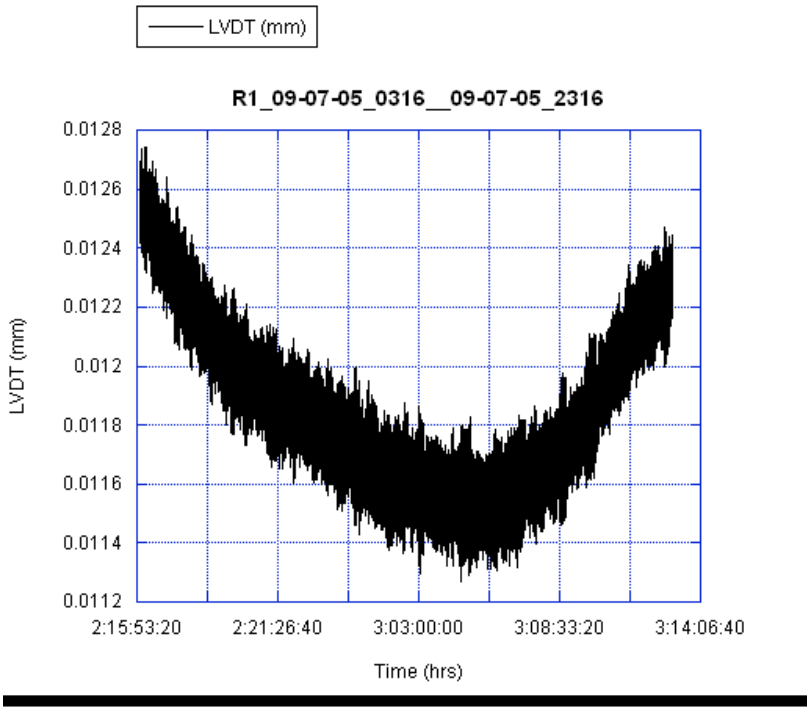

Fourth Quarter of the Data:

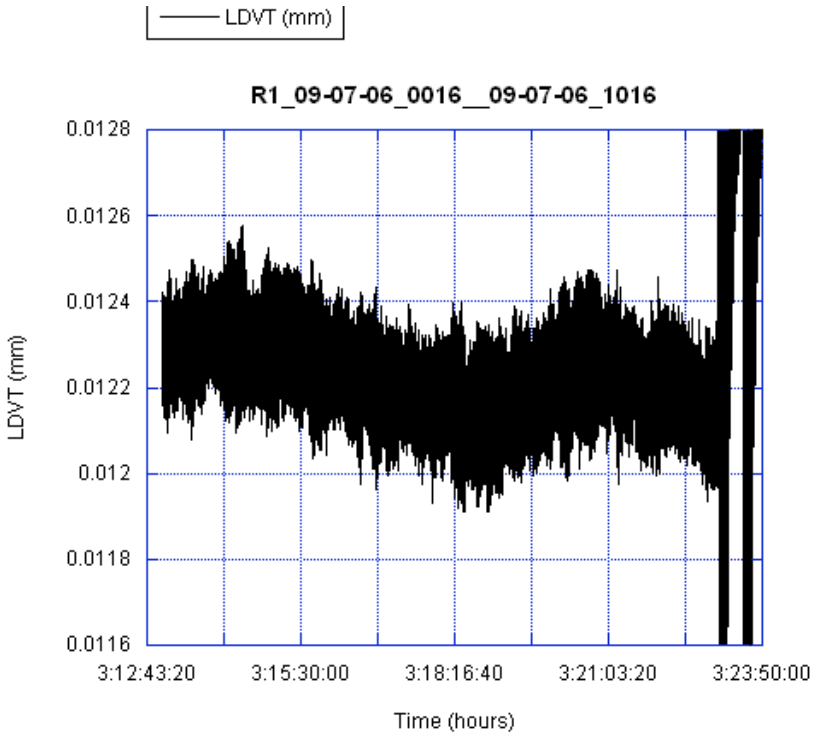

This seems like minor noise that has drifted up and down slowly with overall amplitude of roughly 200 nanometers over a period of around 12 hrs.

It is puzzling that the jumps in the current request (seen below), a “software value” follows a trend that is almost same as the LVDT – possibly an indication that the problem is software-related.

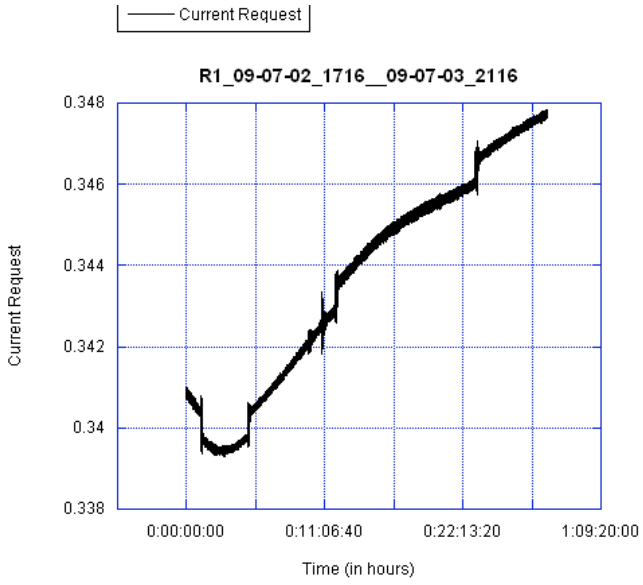

The data analysis will be divided in the following steps:
Study of the trend
Study of the noise around the trends
Study of the jumps and re-excitations

Study of the Trend:

By zooming into the data of the 2nd quarter, it is observed that the width of the data stream is made up of oscillations with the characteristic period (about 10 s) of the tiltmeter.

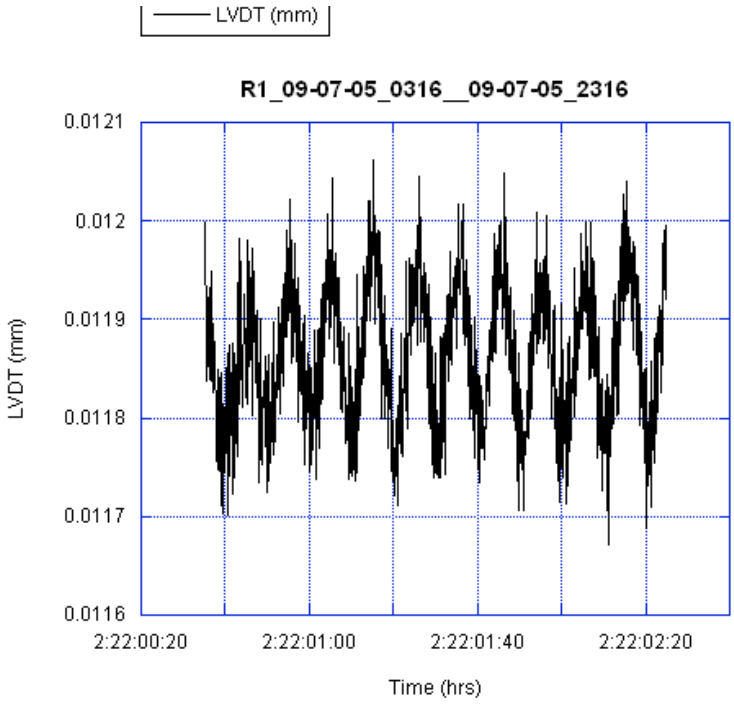

This LVDT oscillation (in this section of the data almost 200 nm) is generated by seismic and ambient re-excitation of the tiltmeter oscillation.
To eliminate these oscillations, we just average the data over an entire period (105 data points) to obtain the trend.

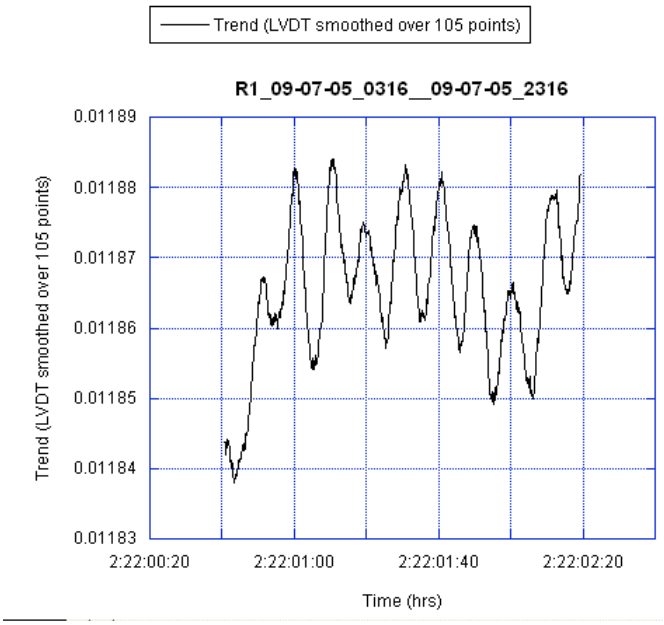

Note: oscillations are erased and the average in this section of data oscillates by less than 50 nm.

Trend of 1st quarter:

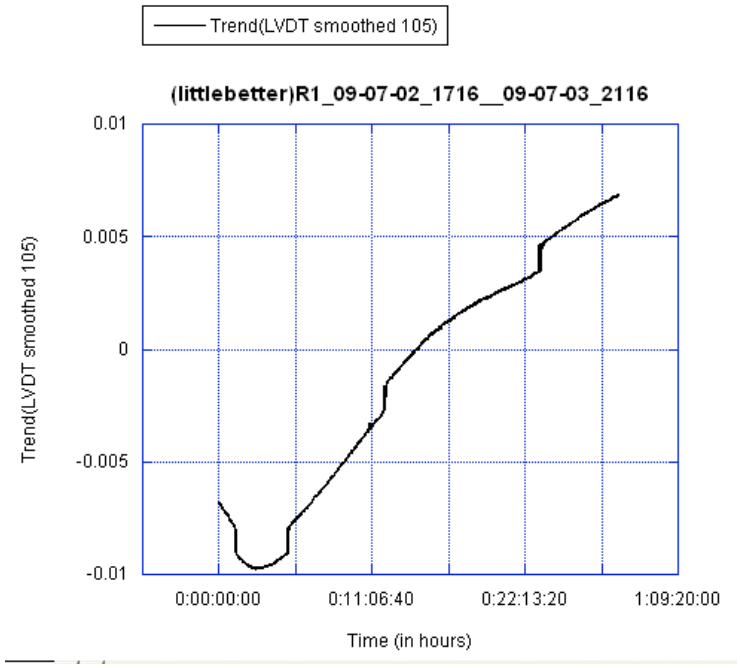

Trend of 2nd quarter:

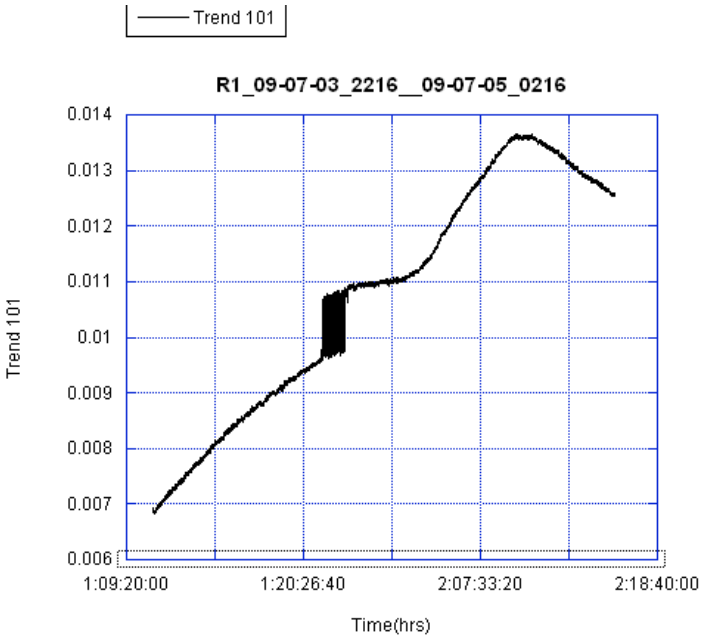

Trend of the 3rd quarter of data:

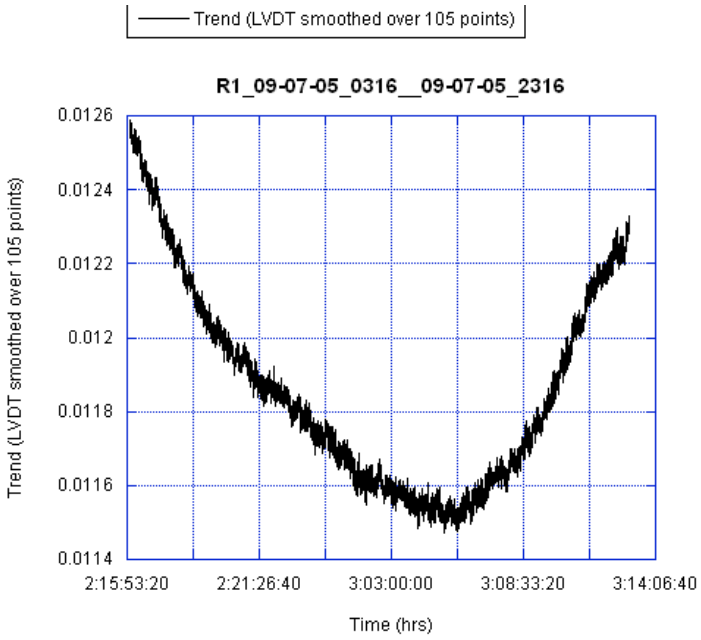

Trend of the 4th quarter of data:

There is a drift going from 12.4 micrometers to 12 micrometers with decreasing amplitude and what seems like a faster period.

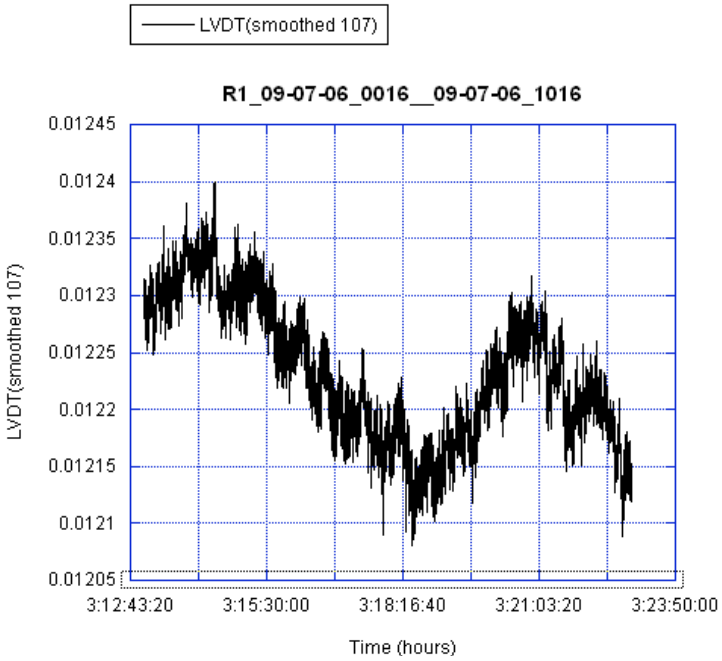

5.2 Study of Seismic Noise Re-Excitation

To study the seismic and ambient noise level, we subtract the trend from the LVDT, which we then called "centered" data. The unit for LVDT measurements is in mm.
Centered data = LVDT – Trend

1st quarter of centered data:
The width of the centered data indicates the daily variation of the seismic and ambient noise that re-excites the tiltmeter.

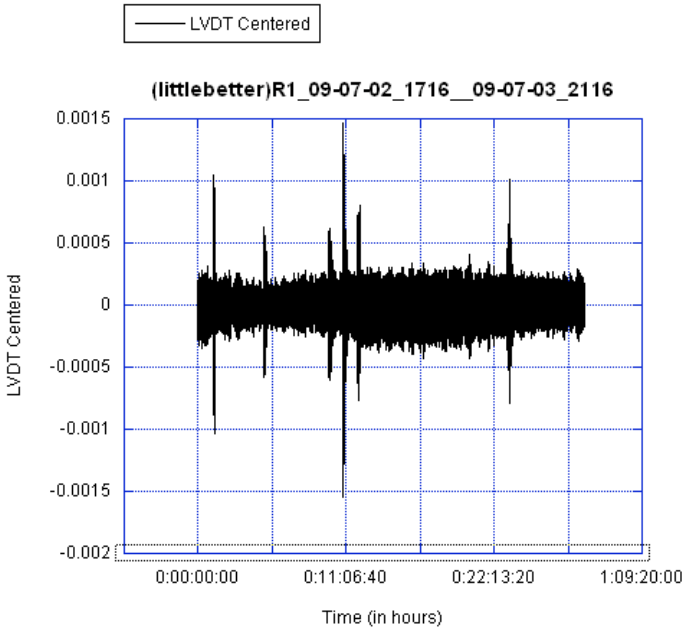

2nd quarter of centered data:

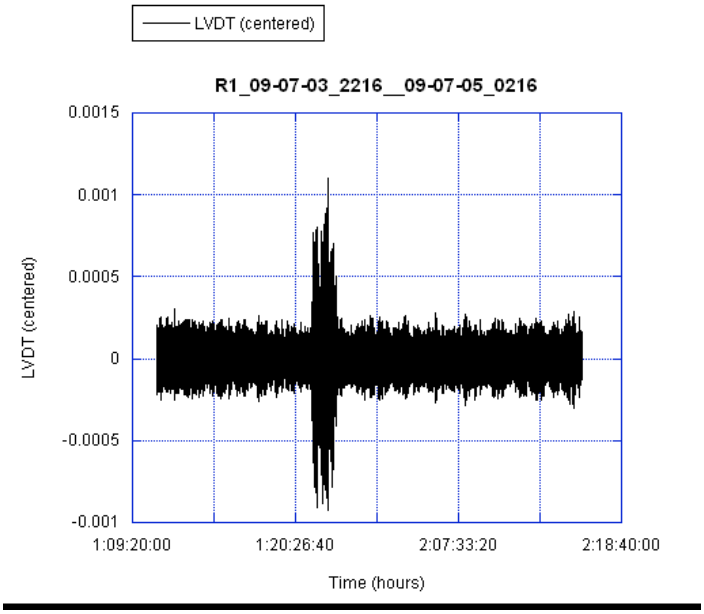

3rd quarter of centered data:
The standard deviation of this data is 6.704382e-05.

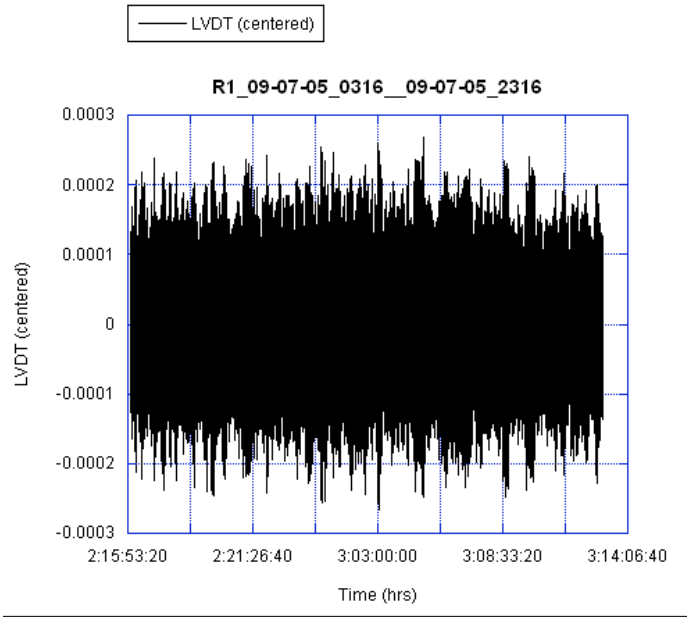

4th quarter of centered data:
The width (from highest peaks to lowest peaks) is approximately 400 nanometers. The standard deviation of this data is 6.7074526e-05.

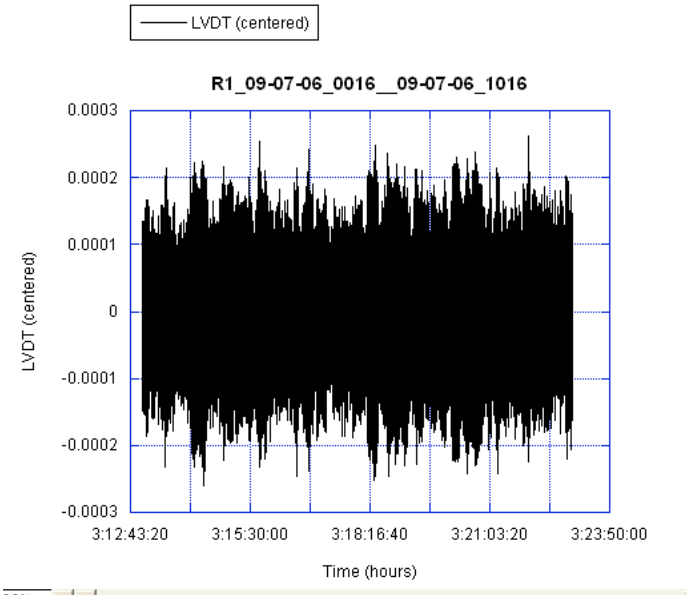

We are measuring how much the tiltmeter oscillates on average because of re-excitation. After "centering" the LVDT data, we get the absolute value of that data and then average it over the same number of points we used when we wanted to find the trend (a whole period). This

gives us a graph that is always above zero proportional to the width of the 'fuzz' of the original data. This is ground noise caused by vehicles on the road, tides, earthquakes, and other artificial and natural phenomena.

1st Quarter Seismic Excitation:

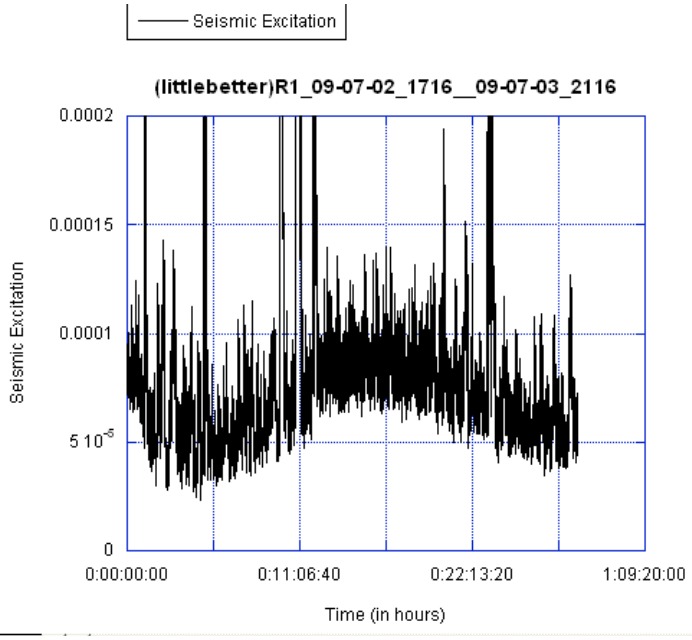

The graph has been cut-off at 200 nanometers because we already know that those occasional peaks that go past 200nm are caused by the re-excitations and unexpected jumps that we have mentioned before and will examine further later.
The system slowly drifts up and down about 50 nanometers. This is most probably because of the shift from day and night. The ground is quieter at night because there are less cars and less activity. The graph above shows data from over a period of an entire day plus a few hours.

2nd Quarter Seismic Excitation:

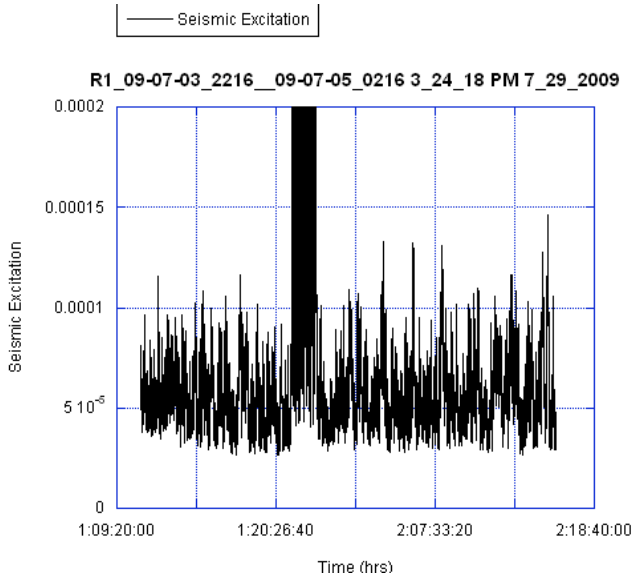

We already discussed that big jump. Other than that we believe there is a slight gradual increase in seismic noise of roughly 30 nanometers. It is a bit more noticeable if one compares the noise before the jump to the noise after the jump.

3rd Quarter Seismic Excitation:

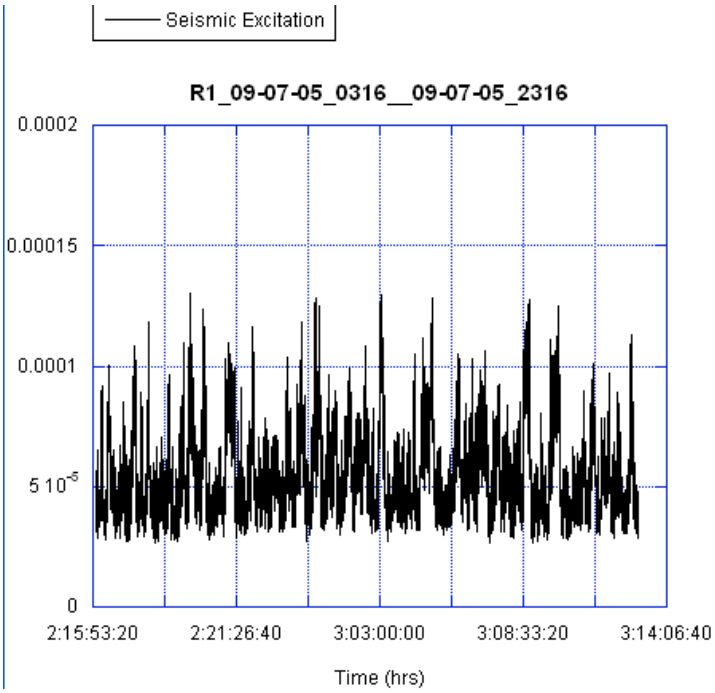

This looks pretty uniform through out. No lab movement, calm weekend data.

4rd Quarter Seismic Excitation:

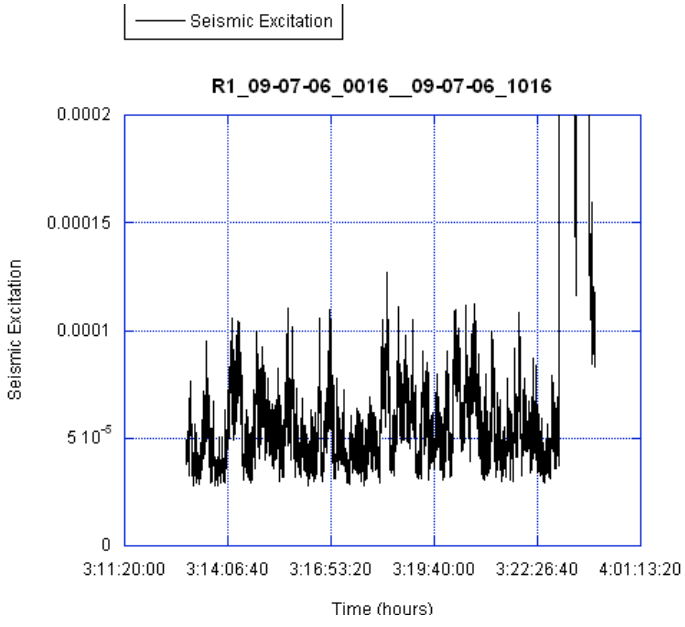

Again, quiet end-of-weekend data before the last two oscillations when lab movement returns. As we can see from this graph, there isn't really anything drastic in the time before the oscillations.

5.3 Study of the Amplifier and Digitization Noise

Since the 3rd quarter of centered LVDT data is relatively quiet, we can use it to evaluate the seismic excitation of the system at a quiet time.

Examining a short stretch of (original and not centered LVDT) data we note that its noise is dominated by the 200 nanometer wide mechanical oscillations at about 0.1 Hz. To evaluate the electronics and digitization noise we need to eliminate the influence of this mechanical oscillation. To do this, first we fit this stretch of data with a sinusoid, and we subtract it from the data to get the residuals, which are essentially the width of the trace, and which will be the electronics noise of the LVDT. We need to do it in a short time stretch, because random seismic re-excitation would cause coherency loss over longer time scales.

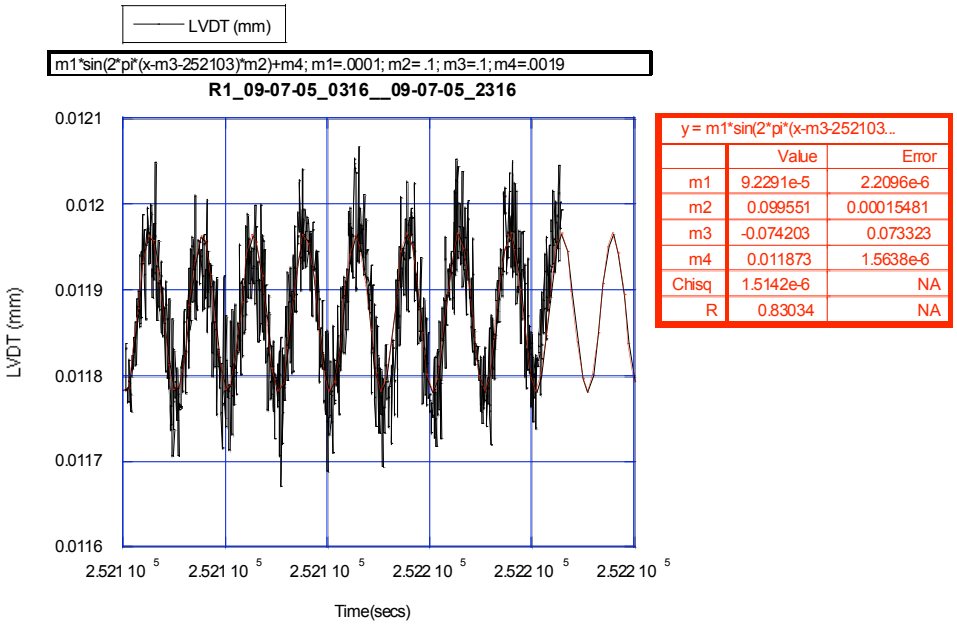

Equation: m1*sin(2*pi*(x-m3-252103)*m2)+m4; m1=.0001; m2= .1; m3=.1; m4=.0019

We histogram the residuals of the sine fit in a frequency mode and fit the data with Gaussians.

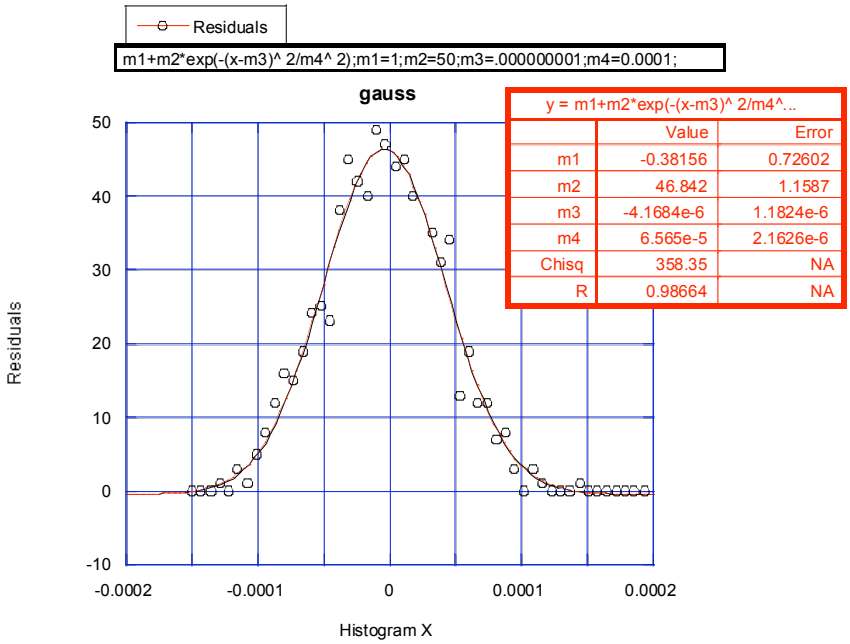

Equation: m1+m2*exp(-(x-m3)^ 2/m4^ 2);m1=1;m2=50;m3=.000000001;m4=0.0001;

The width of the Gaussian is 65 nm, not a bad result considering that the LVDT gain is still low. The subtraction of the sinusoidal mechanical excitation is approximate – because of the continuous seismic re-excitation, the actual electrical resolution may be even smaller. This resolution contains both the LVDT noise and the digitization noise. The 16 bit digitization noise over the ±10 readout range is 20 / (2^16 √12) = 88 nm per sample.

5.4 Study of the Discontinuities and Jumps

1st Quarter Coil Driver 1 Output:

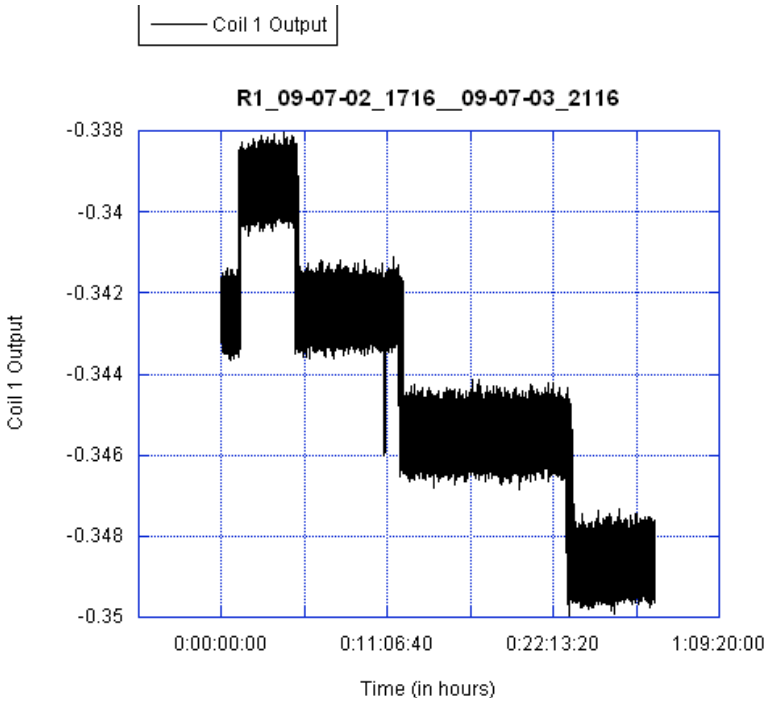

There are 4 distinct jumps. There seems to be an irregularity, (jump) corresponding to the jumps observed in the LVDT channel, as can be seen by comparing the above graph to the one below.

This would seem to indicate that it is a jump in the coil current to generate the jump in the LVDT data. This makes little sense though, because a step should be followed by a normal ringdown, which we do not observe (see detailed analysis below). Therefore we consider the step an event of data acquisition software.

We remind that that the feedbacks are off, and the Digital to Analog Converter generating the coil driver voltage is not expected to generate any step.

Coil Driver 1 Input:
We see some smaller jump also in the coil driver 1 input voltage, incompatible with what observed after the driver.

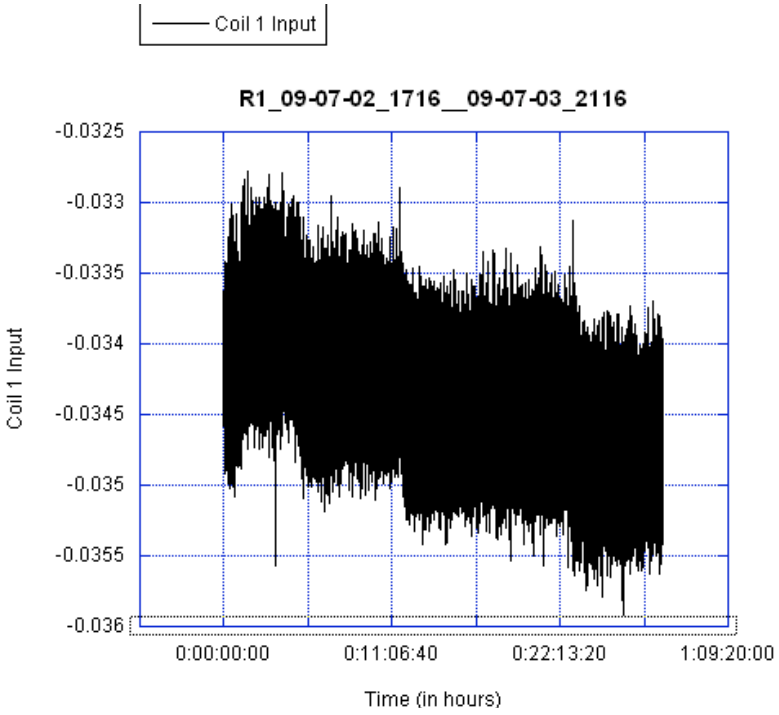

1st Quarter Coil 1 Output smoothed over 105:

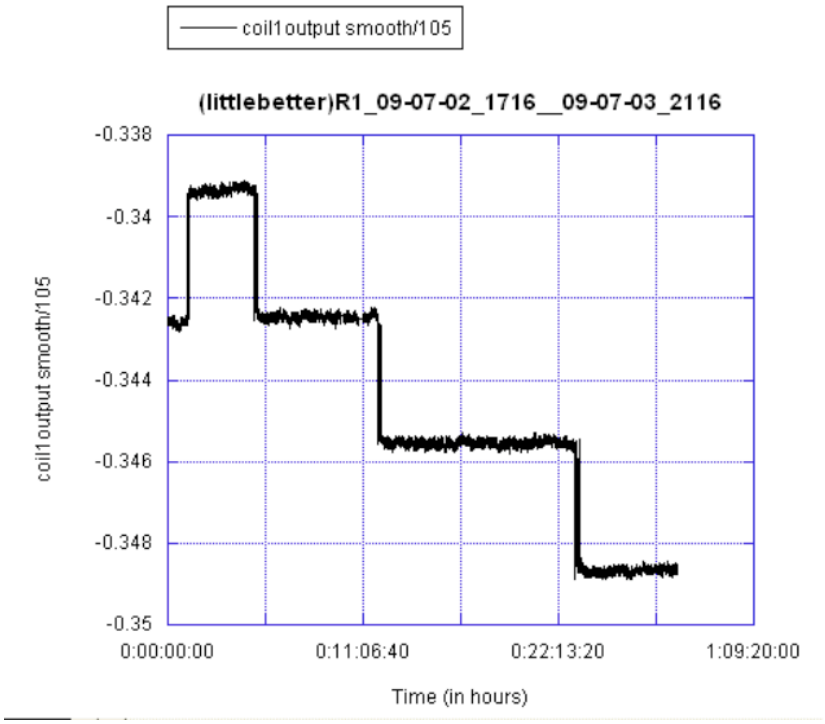

1st Quarter Coil 1 Input smoothed over 105:

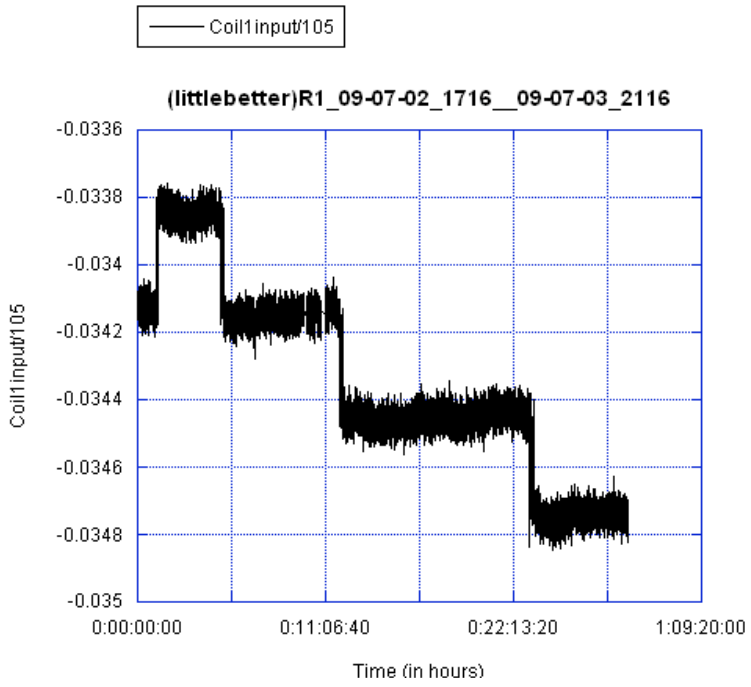

It looks like both the input and output have jumps that occur at the same time. In fact, the graphs look almost identical save for the fact that the Input is a lot noisier, which gets quieter when the current comes out in the Output.

Coil Driver 2 Input:
Quiet throughout, even during the jumps of other channels, unlike Coil 1.

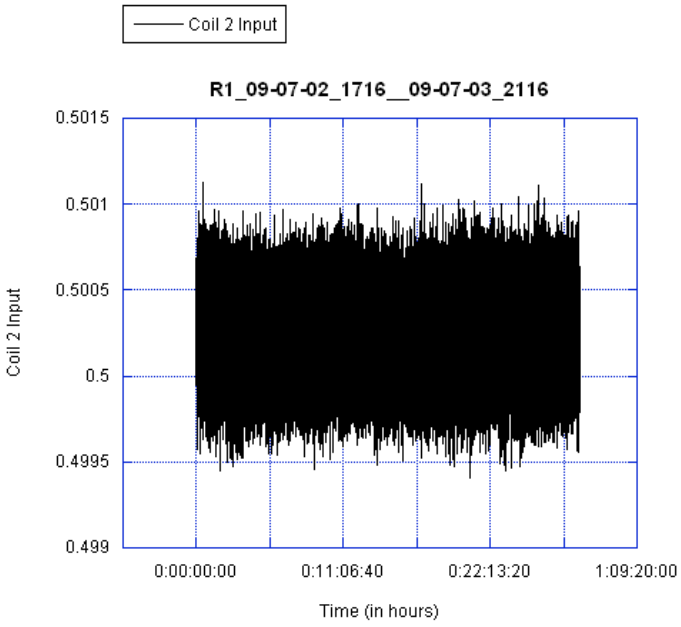

Coil Driver 2 Output:
We notice that the coil input has jumps, while the coil output is quite stable. We note only a very a small slope of about 1 mV (over the ~5V value) of the amplifier output, which is probably a thermal drift of the amplifier.

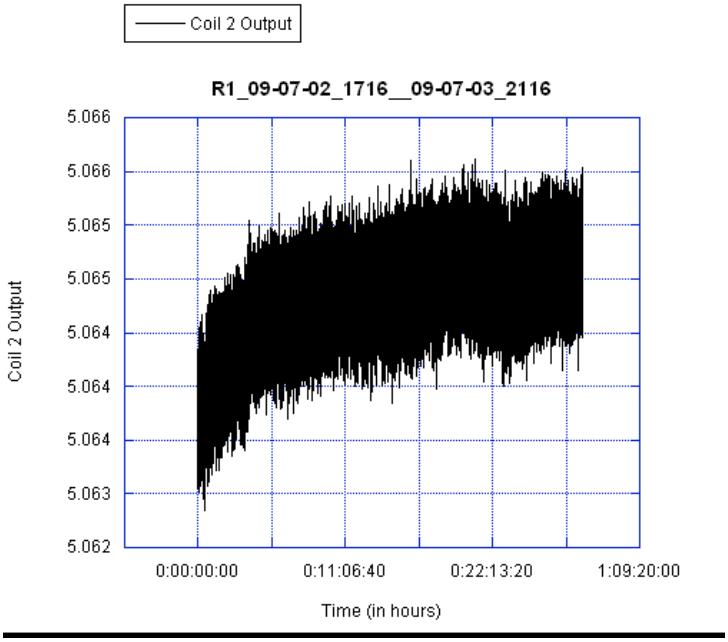

LVDTs at the Jumps:
The LVDT data appears unphysical, the oscillations start and stop abruptly, without the characteristic mechanical ringdowns.

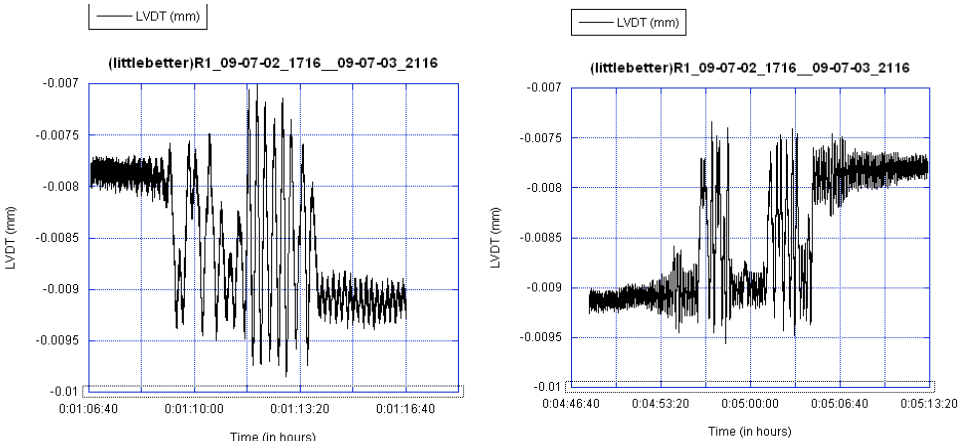

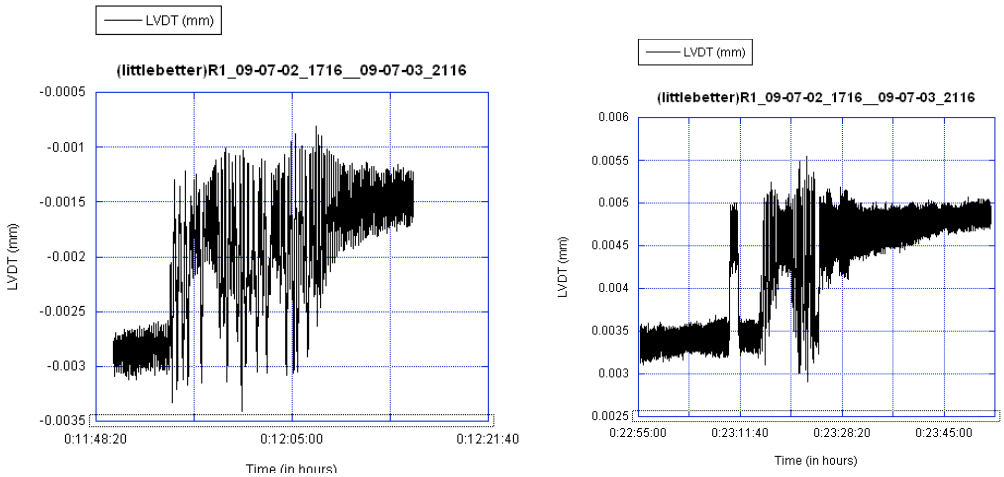

Study of the jump in the second quarter:
It is accompanied by large instabilities and followed by larger noise in the coil driver input and output signals.

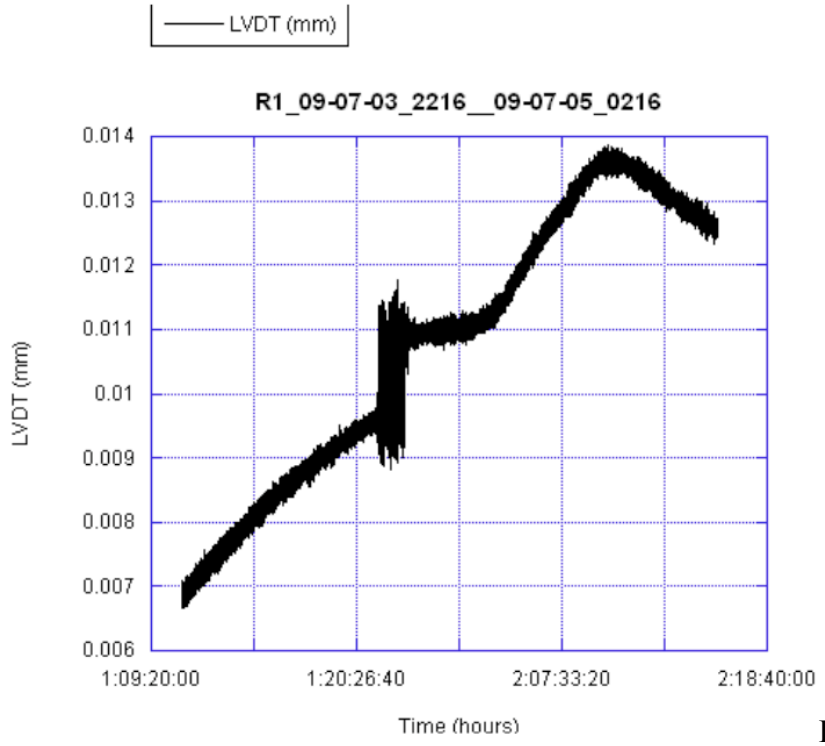

LVDT plot

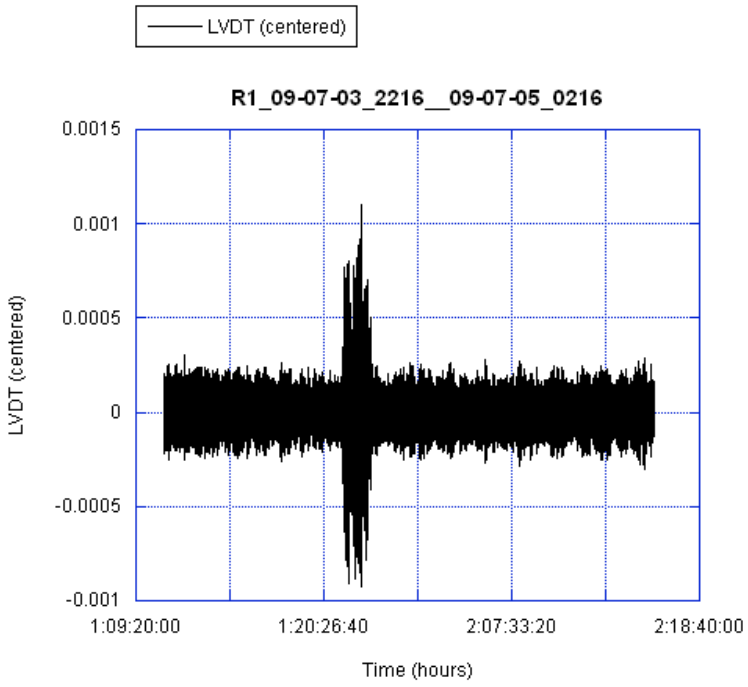

The Centered Data

In the input and output signals of the two coil drivers we observe mainly much larger electrical noise in all channels after the event, as well as a jump in coil 1 output. Note that the noise appears in coil 2 input "before" than in the other channels.
This again does not look physical, possibly electrical, more likely software connected.

Coil 1 Output:
There is a huge change in width after a jump. We do not know what caused this.

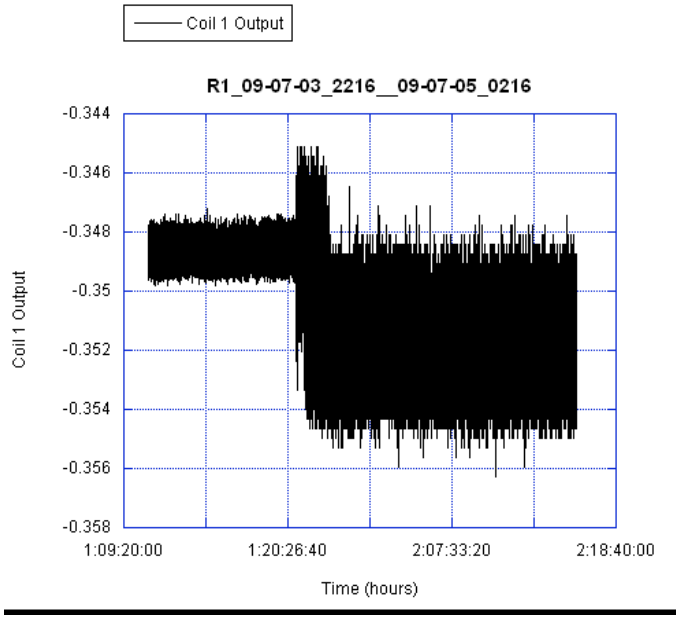

Coil 1 Input:
Around the same time as the big change in the Output, there is a huge change in width, but no jump, just a sudden change in noise level without change in average value.

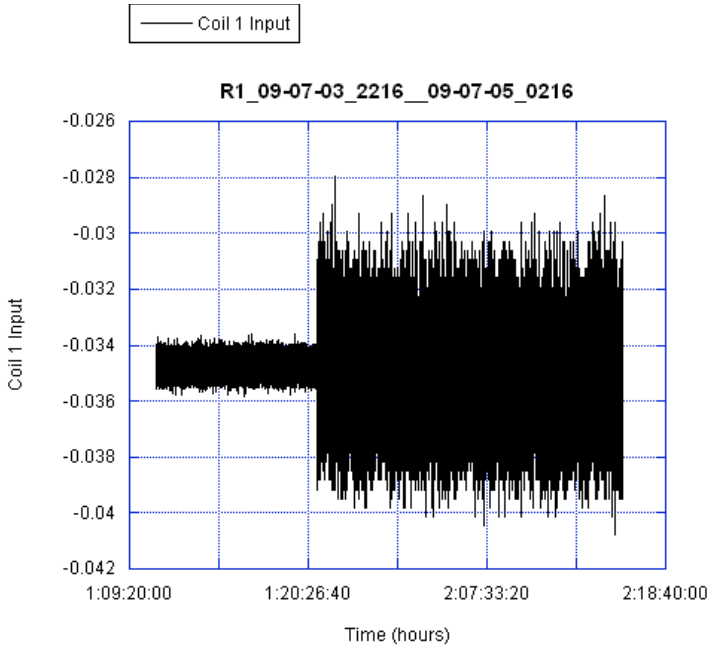

Coil 2 Output:
Again, a big change, but this one drifts down and up slightly of about 1 micrometer.

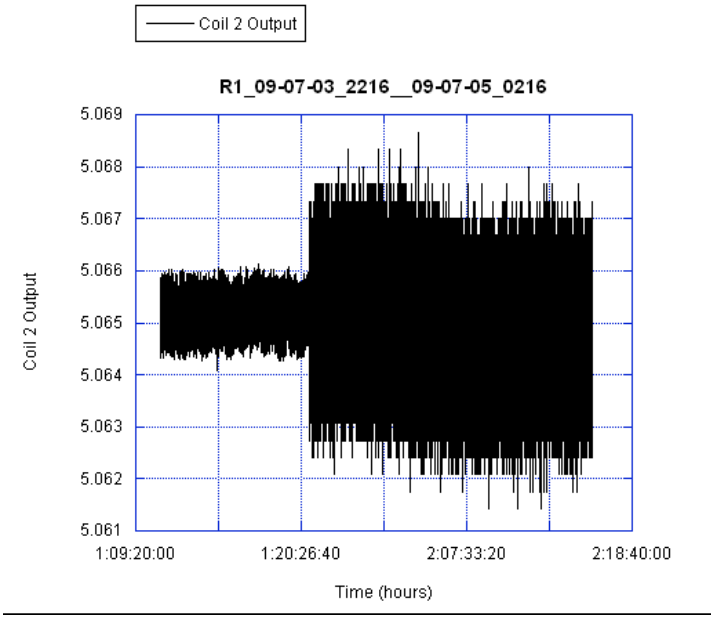

Coil 2 Input:
Interesting to note, the Inputs seem very similar to the Outputs, save for a mysterious part of the data that showed up in the Input but not in the Output.

Study of the Two Re-excitations in the First Quarter:
These seem much more physical perturbations ringing up the system that later decays normally. Note that these perturbations do not disturb the trend.

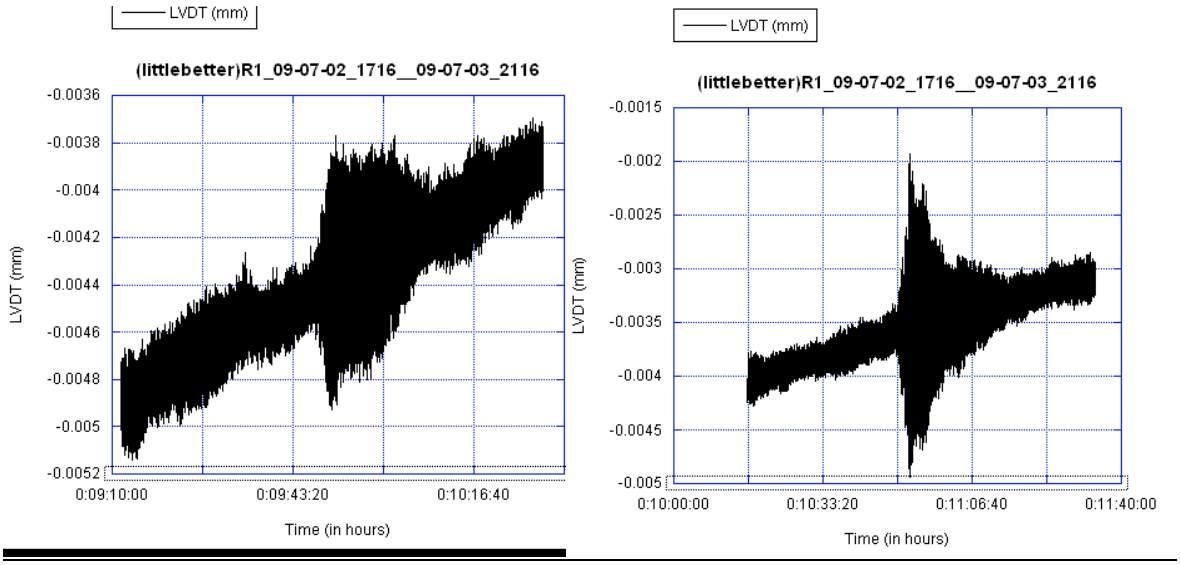

Study of the Two Re-Excitations in the 4th Quarter:
The two re-excitations at the end of the data set seem quite physical. We notice in both cases a ringup of only 2 cycles. Otherwise they seem normal happenings. They are likely an experimenter-induced excitation, as shown by the kick in the coil 1 channel. They are not interesting, except for the fact that the very regular excitation and disexcitation pattern highlights the not normal and unphysical (software or data acquisition generated) behavior of the jumps studied earlier.

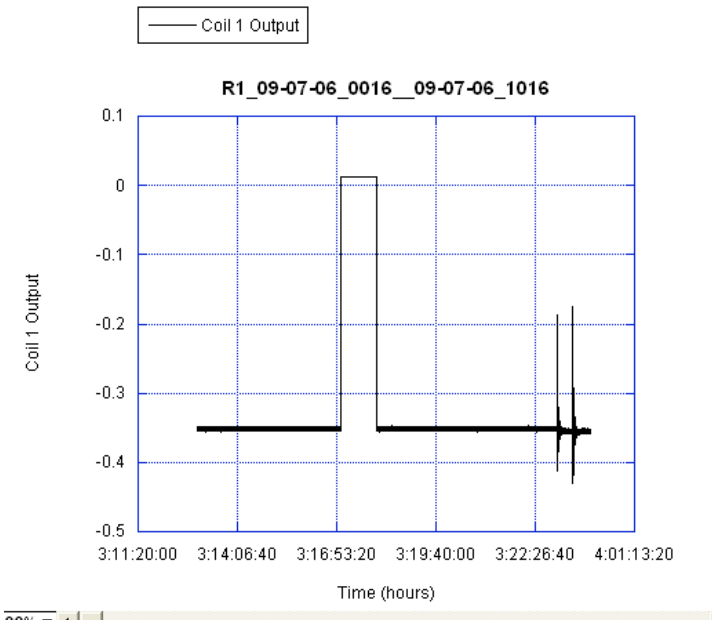

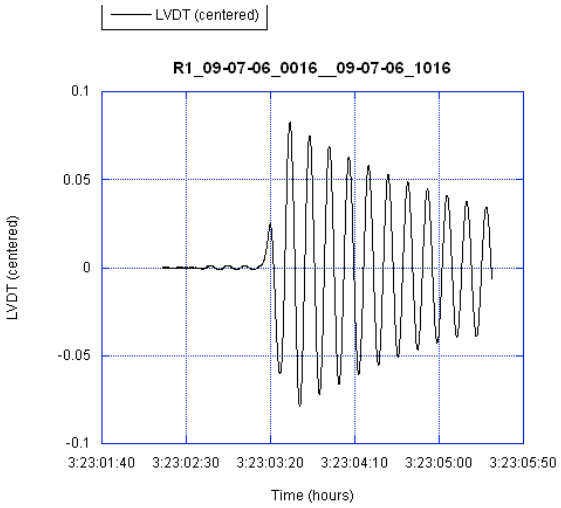

Beginning of first oscillation

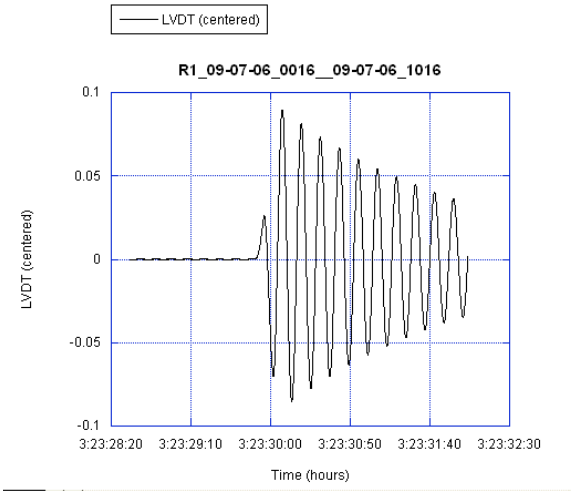

Second oscillation

Coil 2 Output of the entire 4th quarter of data:

Steady until it begins to slide down 1 micron (1e-06 m), possibly from thermal drift.

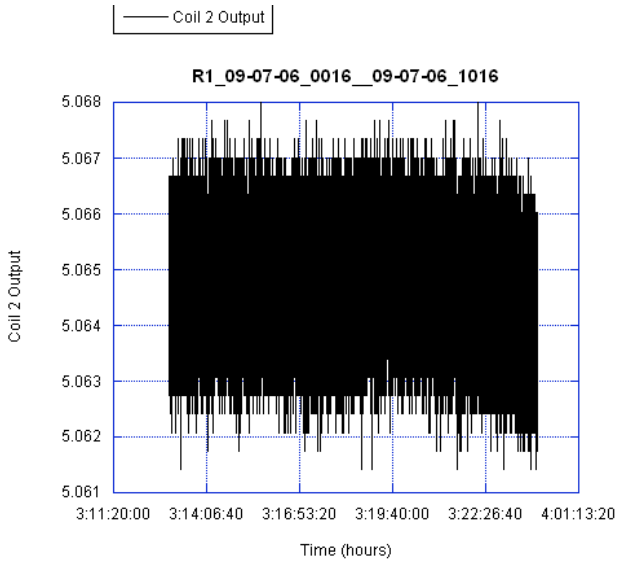

Coil 2 Input of the entire 4th quarter:
The graph thins as it approaches the last two excitations.

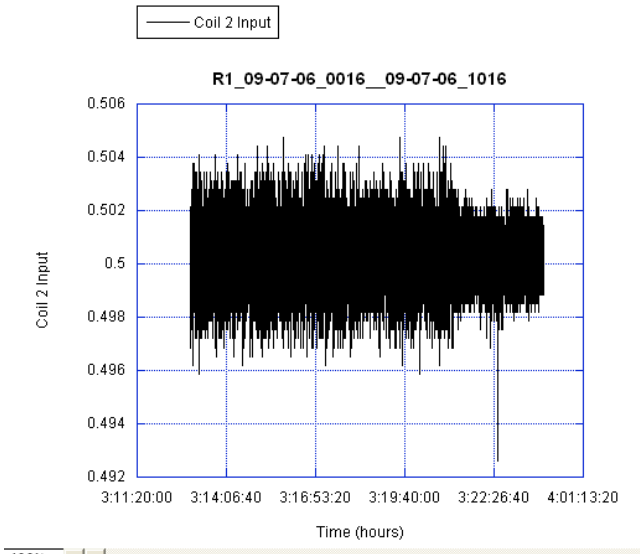

Overall Seismic Excitation:

We want to see the entire overall seismic excitation in one graph. For that we are take a point of data every 10 points from the seismic excitation graphs of every quarter of the weekend data and put it all in one graph so we can see the main changes in seismic excitation throughout the weekend.

The y-maximum is 1 micron. There is an interesting exponential growth that suddenly falls off three times. Because of night and day, we expect a slight oscillation over time.

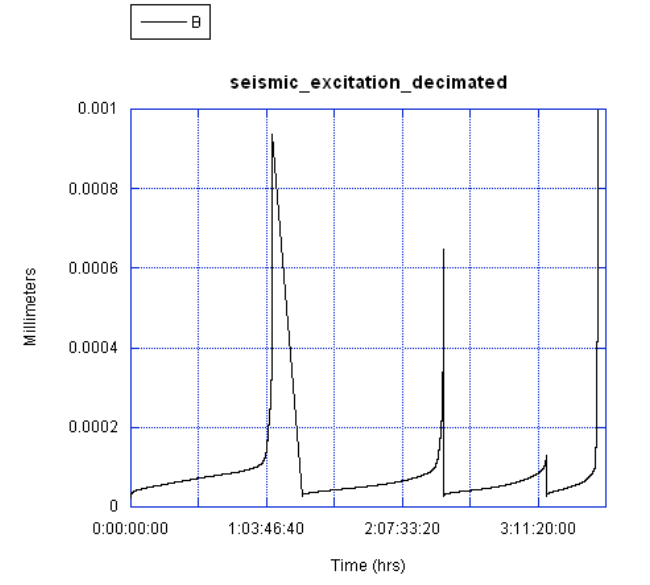

6 System Noise Analysis (Part II)

We took data over another weekend, from the evening of August 7 to the morning of August 10, with all feedbacks off (zero EMAS gain and no position integrator) to test the mechanical stability of the tiltmeter and the stability of the acquisition program. The data was acquired by the new Lab View program made by Gong Pu and Andrey Rodionov. Because of this new program, the data tables are a bit different and the data itself is much denser.

The acquisition of this new program included the following channels:
1) Integrator
2) Actuator
3) LVDT (1+2) – position of left side + position of right side of arm
4) Coil Current
5) R. Coil Current
6) LVDT (mm)
7) EMAS Gain (set to zero)

Because of the great amount of data, and the limited capacity of the Kaliedograph tables, the data had to be divided into six parts. The time has been converted from seconds to Days, Hours, and Seconds. In each graph data **Time=0** corresponds to **5:57 PM** on **August 7** when we started acquiring the data.

The time is reset to zero and the integrator value is fixed at -0.39782, so we can throw away that column, which has no value.

We can also discard the actuator request value, which is 0.39782, and the EMAS gain, which is zero. The time step is 50 ms/data point.

Coil current request statistics:
Minimum -0.40428099
Maximum -0.39277899
Mean -0.39965349
Std Deviation 0.00092075139

We note that it has a standard deviation of 0.9 mV.

Binning the data one sees clearly the ADC bit structure:

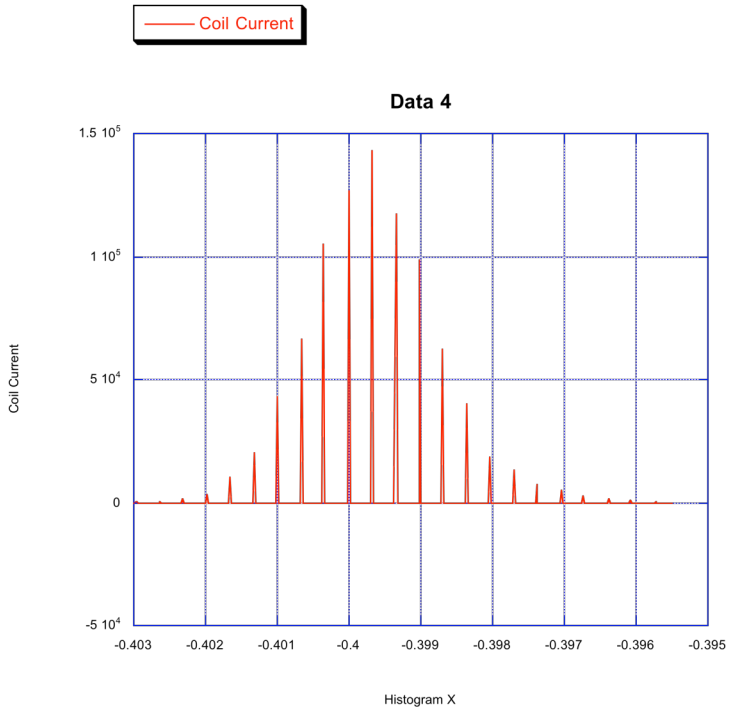

We note that the bin width is 0.32 mV, dividing by √12 we get the digitization noise 0.092 mV, approximately 0.1 mV. We eliminate the zeros from the histogram and replot, fitting with a Gaussian, the width is 1.1 mV compatible with the statistics estimation of 0.9 mV.

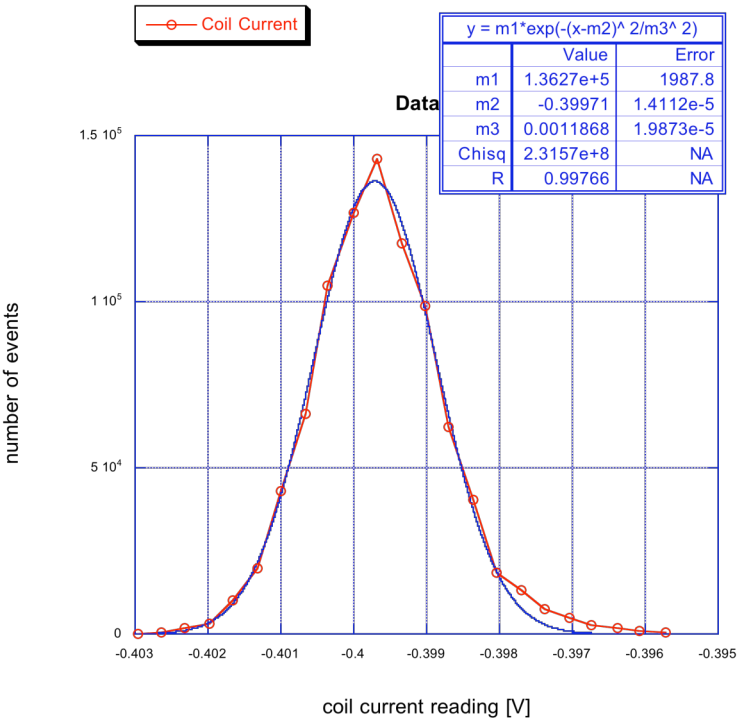

Coil current readback:

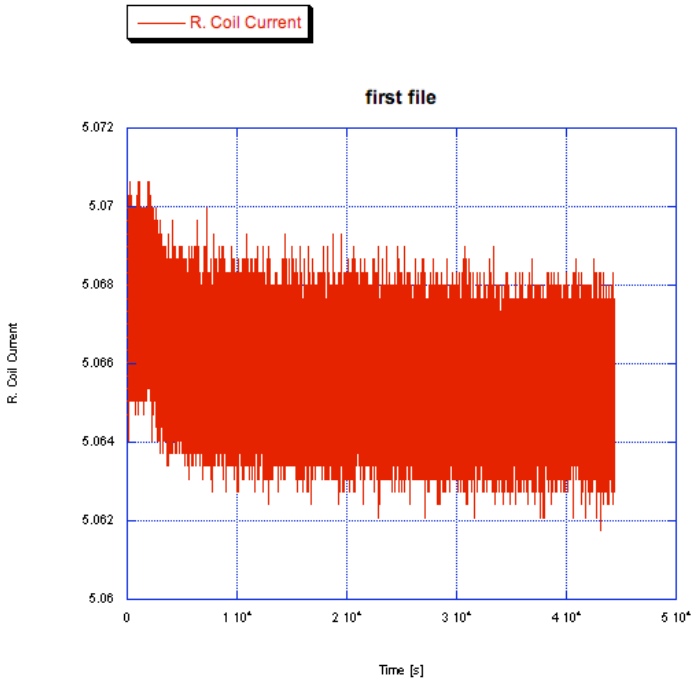

We notice that there is an initial residual drift, which is not visible in the coil current request. Therefore we mask off the first 10,000 seconds and remove it.

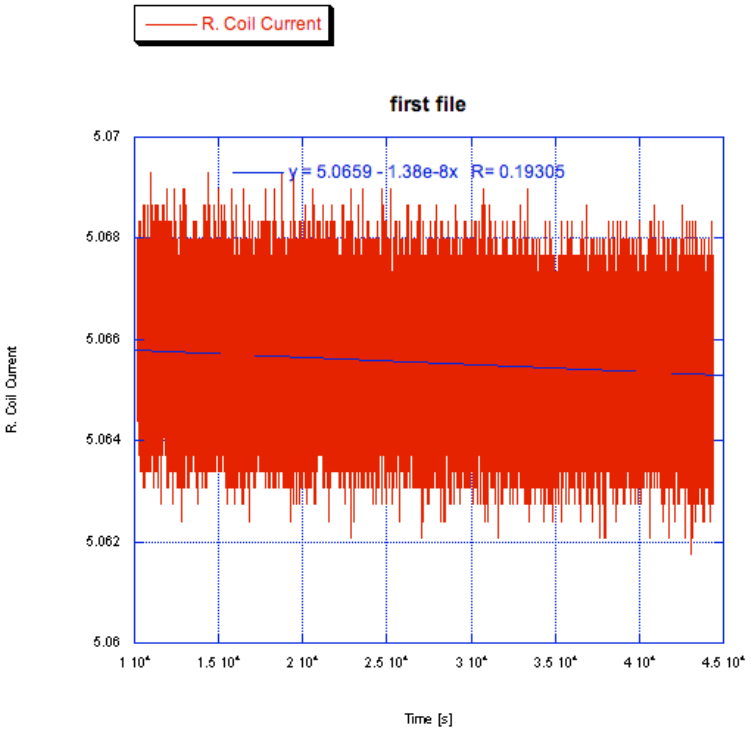

The residuals from the linear fit show the following statistics:
Minimum -0.00366
Maximum 0.00357
Points 684505
Mean -4.2255055e-16
Std Deviation 0.00069

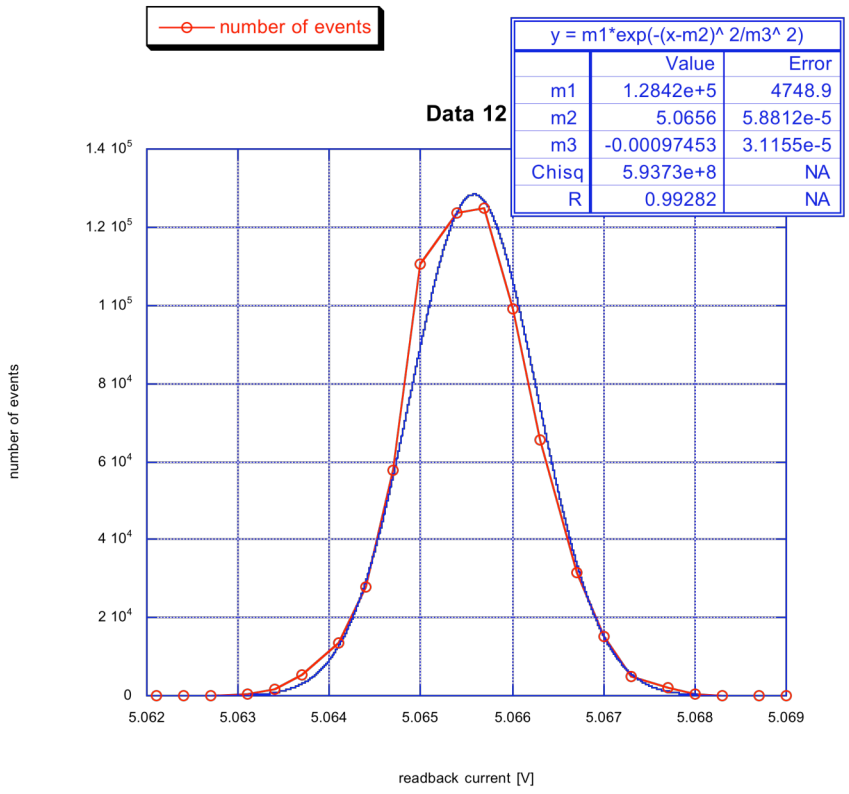

The standard deviation of the current readback, after the amplifier, is 0.7 mV, less than the current request. Binning plotting and Gaussian fitting yields 0.97 mV noise (it is not multiplied by 10 by the amplifier). Therefore the noise of current request is all readout noise.

The LVDT (1+2) shows a similar initial slope, then stabilizes, but at ~32,000 seconds it has a burp, then returns to the original point.

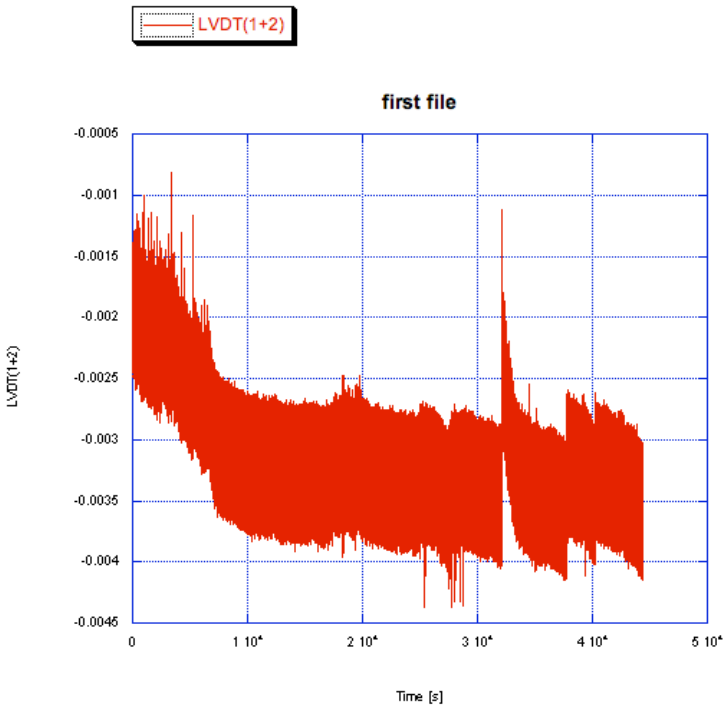

LVDT difference (in mm):
The data is taken at a 50-millisecond interval, much faster than the movement we want to study. It is therefore useful to average over 21 points (1 second). This smoothing reduces the error but preserves the oscillating motion reading, which is 16 seconds long (0.062 Hz).

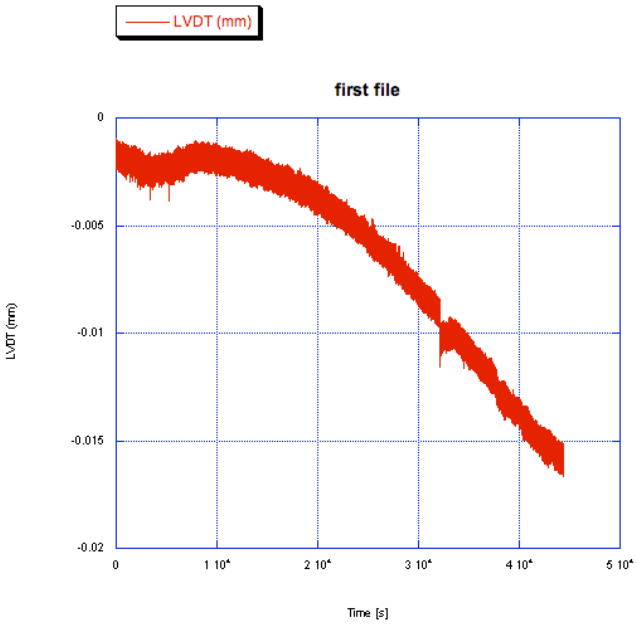

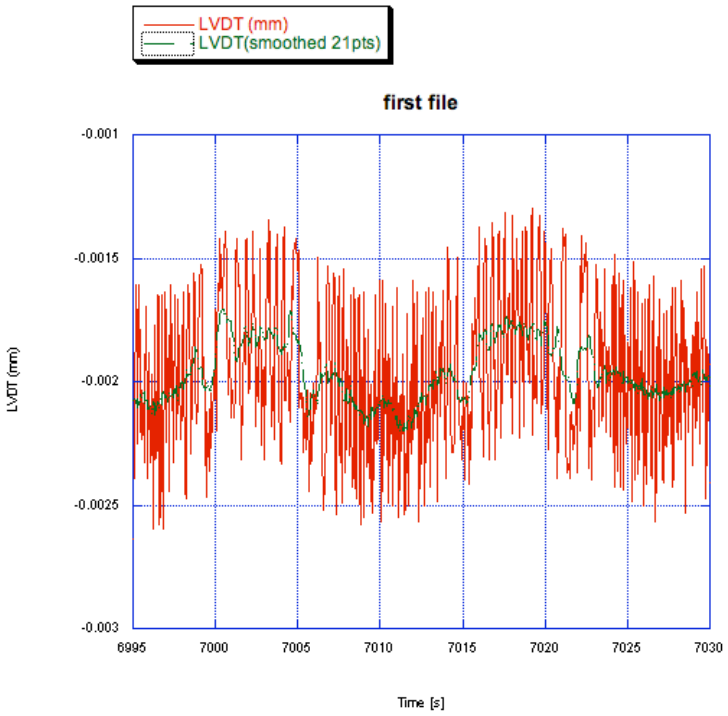

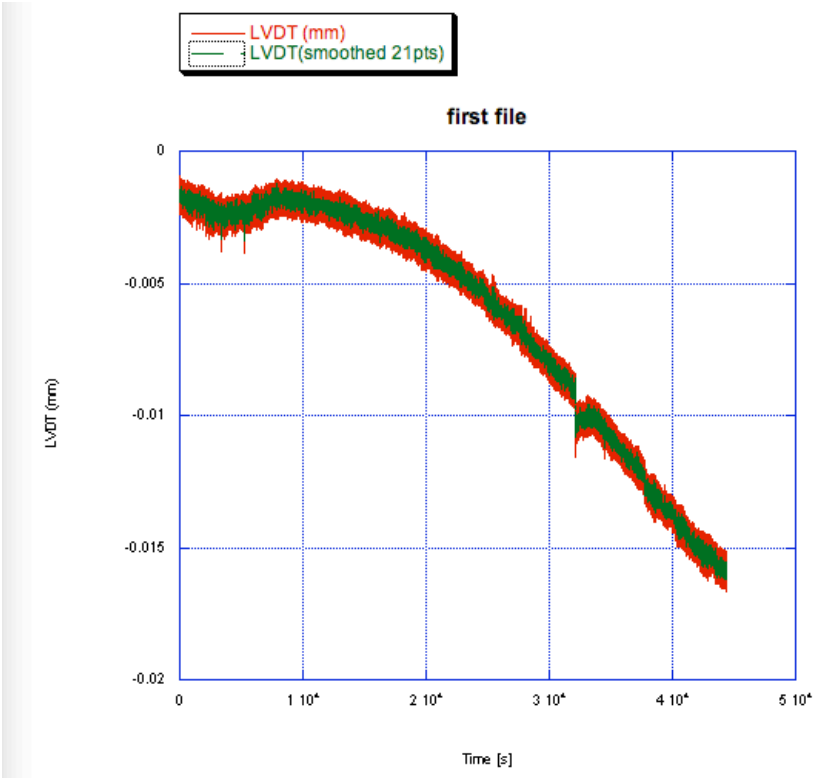

We notice the same glitch at 32,000.

It is now useful to study the trend, to do this we average over a period.

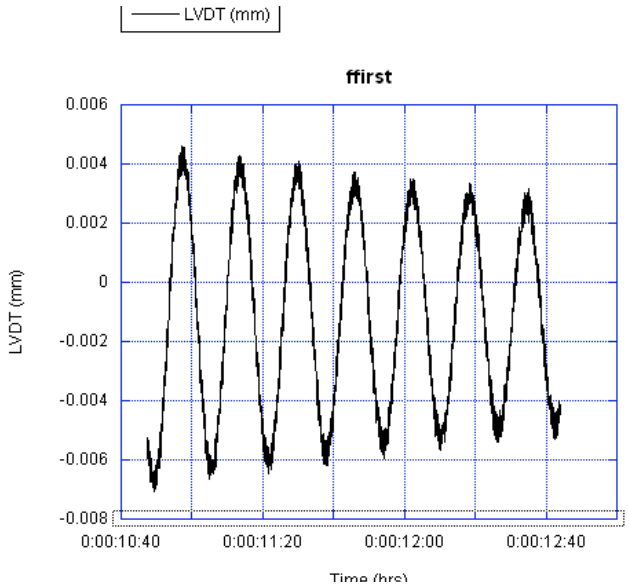

Zoom-in of beginning Oscillation

By smoothing over 329 points (a typical mechanical oscillation period), we get the trend.

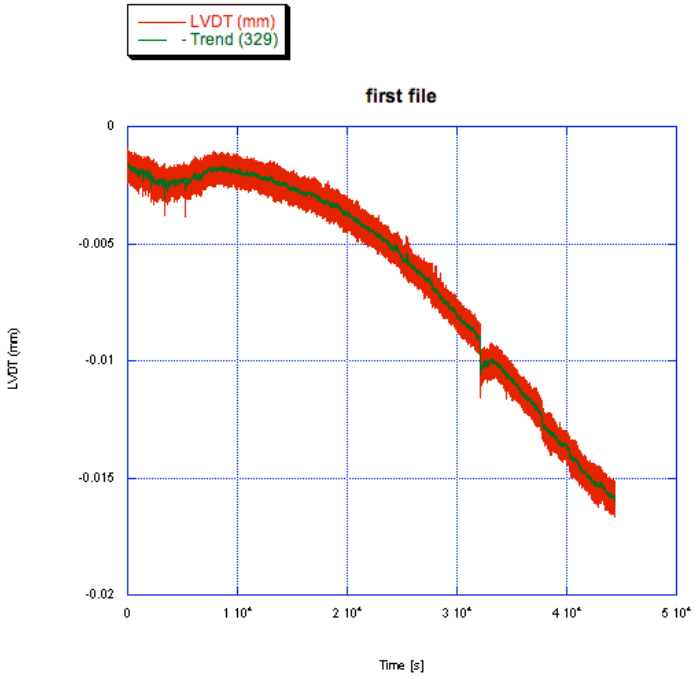

By subtracting the trend, we get the flattened LVDT, which should represent the seismic and ambient excited oscillation.

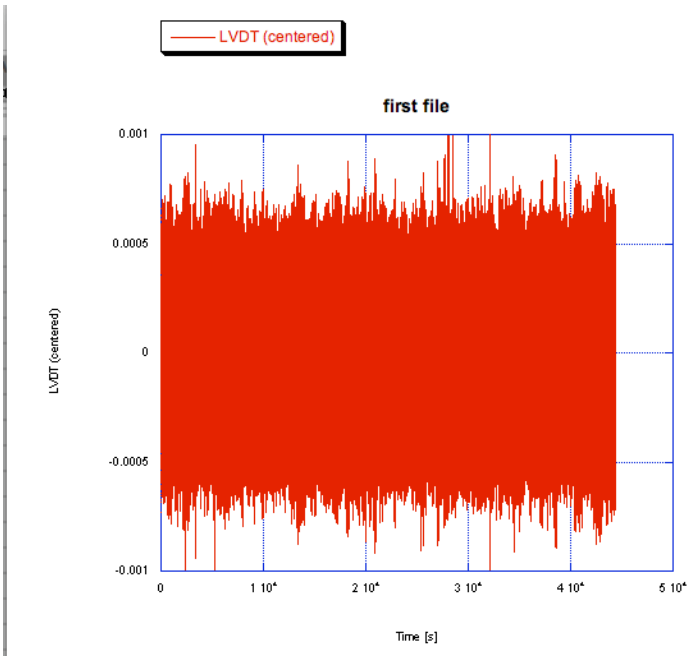

It is still very noisy, therefore it is useful to average it over 21 bins (1s), this will reduce the digitization noise by $1/\sqrt{21}=0.22$.

	LVDT (centered)	LVDT (centered-averaged)
Minimum	-0.0018097628	-0.00082666083
Maximum	0.0012527993	0.00083202851
Mean	-7.6261703e-10	1.4289864e-10
Std Deviation	0.00030590825	0.00011929901

0.3 micron mean oscillation.

Note that the RMS reduced by 1/3, therefore the digitization noise was likely dominating the oscillation motion noise.
We get a snippet of data and fit with a sinusoid and find a period of 16.6 seconds.

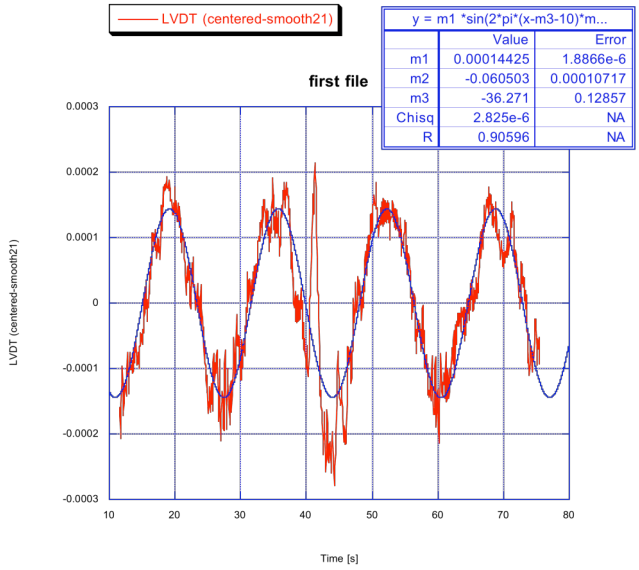

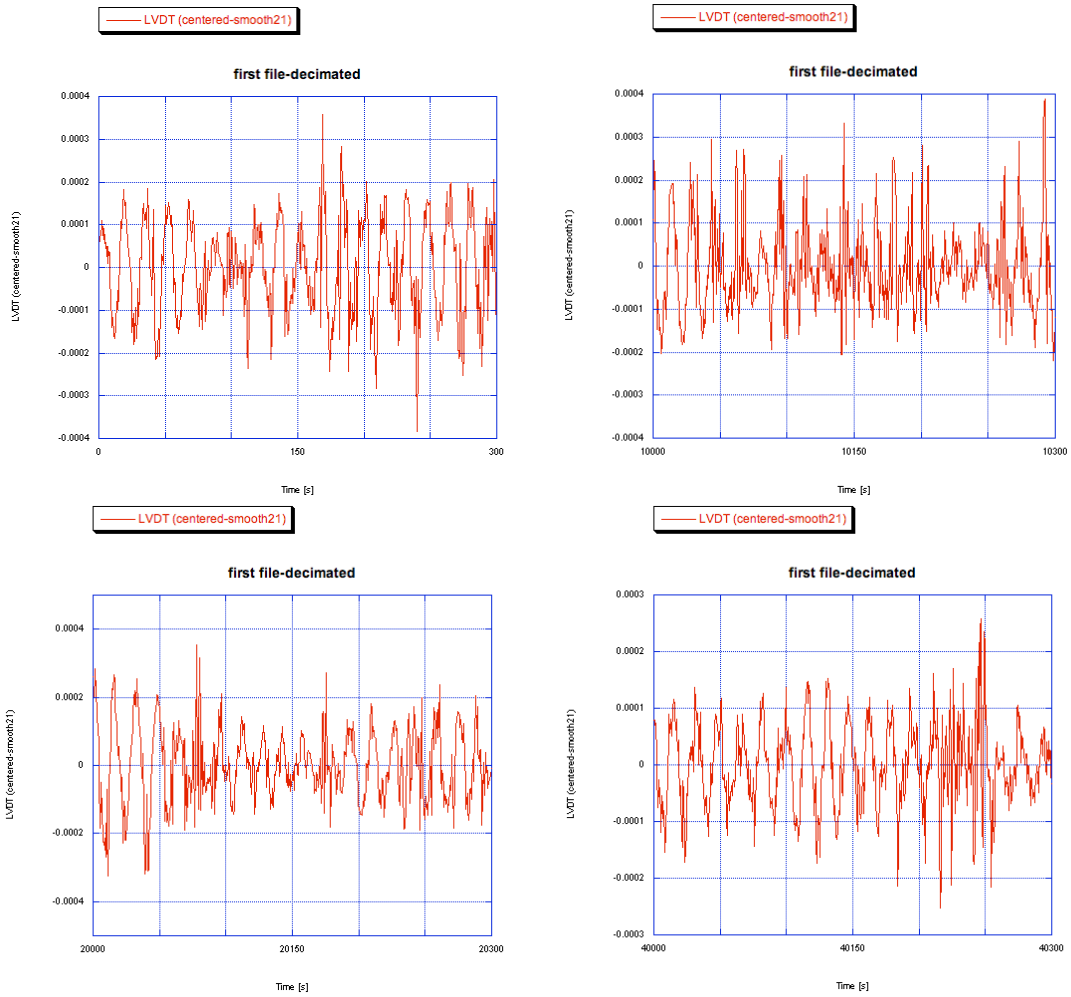

In a snippet where it seems more regular we make a sinusoid fit.

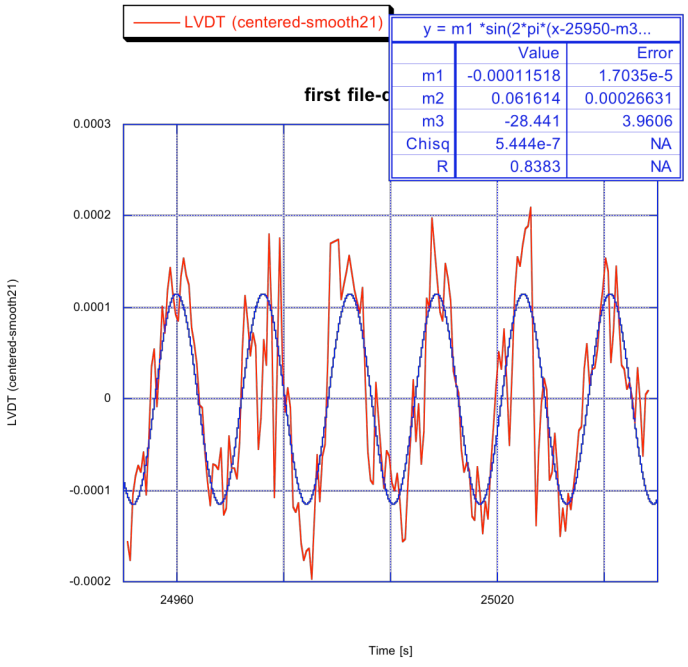

The residuals indicate:
Minimum -0.00014702872
Maximum 0.00020437147
Mean -1.5620962e-06
Std Deviation 5.3225383e-05

Note that the digitization noise evaluated above was 92 nV, which averaged over 21 points would give 20 nV digitization noise in absence of systematics. The digitization noise is contributing substantially, if not dominantly.

6.1 Study of LVDT

First of Six:
The Oscillation at the beginning of the acquisition was probably lab movement before the weekend. The noise in the system has a constant width of noise of about 1.5 micrometers. The overall LVDT seems to gradually drift below zero, probably caused by another factor we are yet to measure.

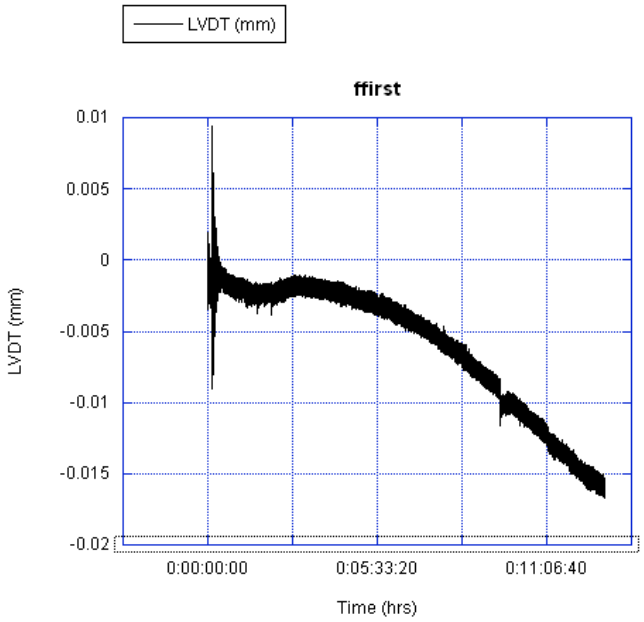

Second of Six:
The LVDT continues to slide down until it reaches -30 micrometers when it begins to go straight.

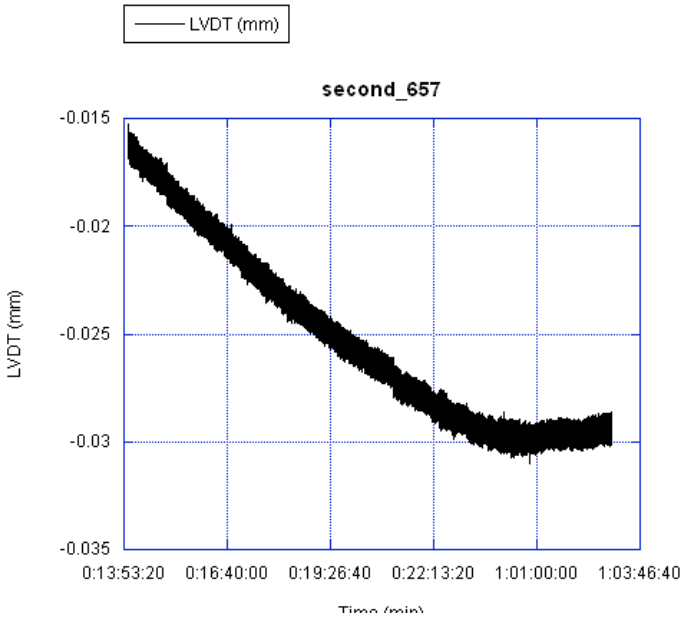

Third of Six:
After several hours of what seems to be steady LVDT with a width of 1.5 micrometers the graph continues to go down at a steady slope.

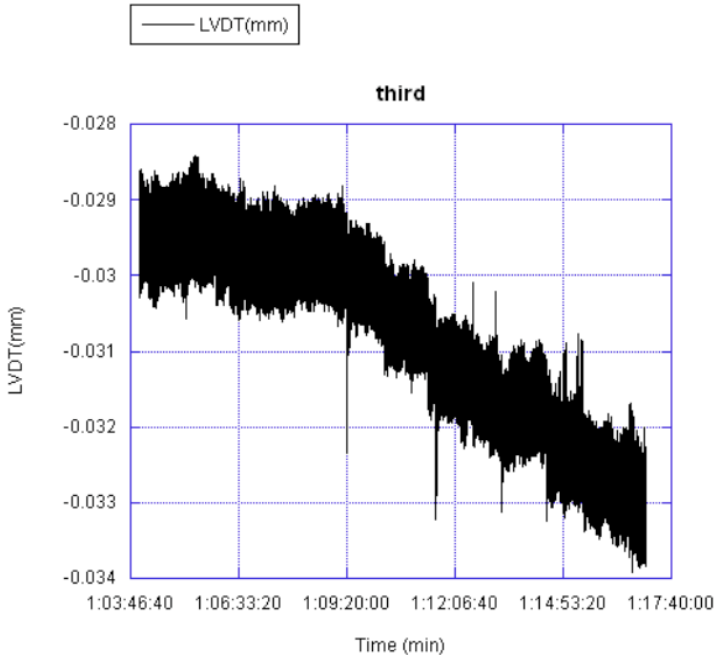

Fourth of Six:
The data is not going down anymore but it seems less smooth and more irregular.

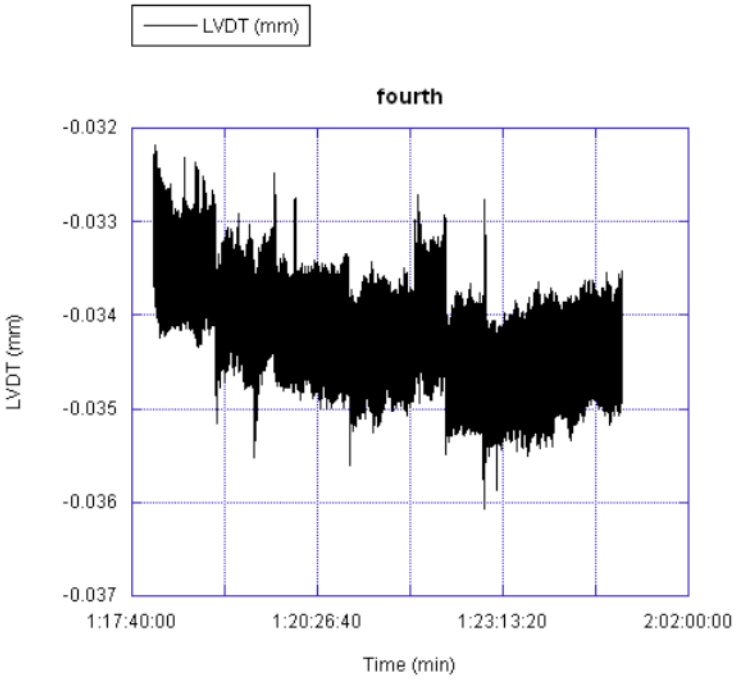

Fifth of Six:

So this LVDT keeps going up and down with a constant width. At this point a decimated LVDT would be useful.

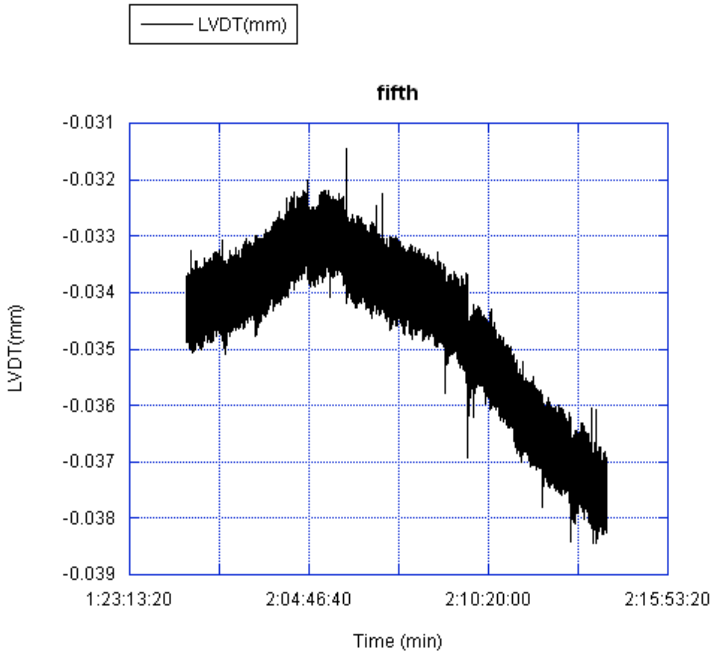

Sixth of six:

Similar data as before, a steady stream of LVDT of width a little over 550 nanometers.

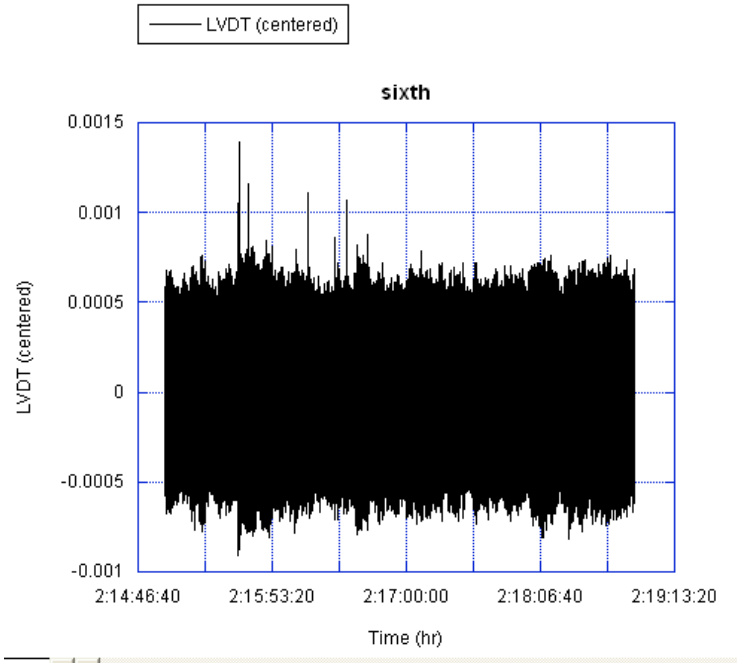

Analysis of the six LVDT files:
The most notable point is that the trend seems to be choppier in the second day (left), while little activity is visible in the "flattened" LVDT signal (right).

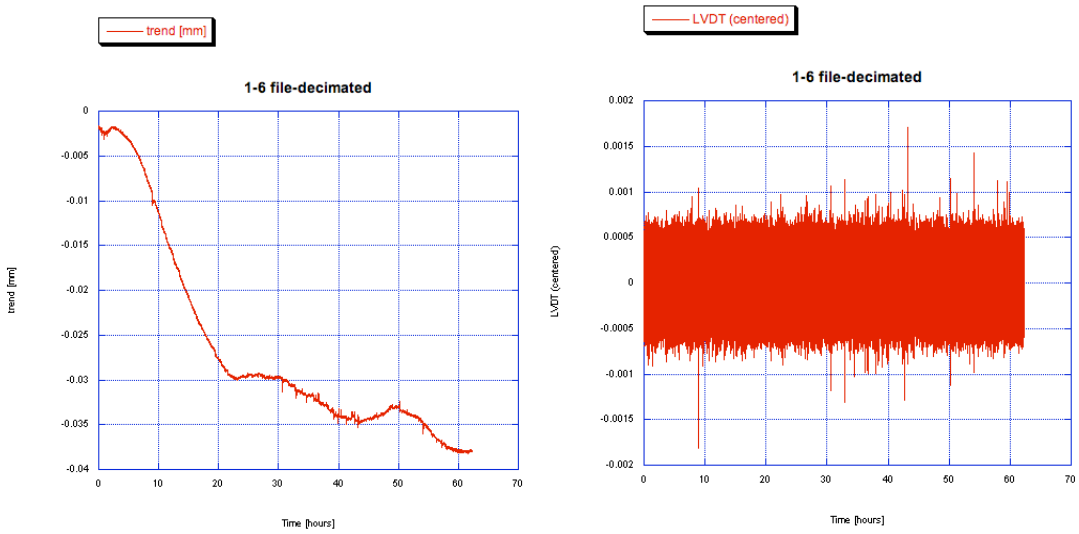

After decimating all six files and merging them we examine LVDT, LVDT smoothed over 1 second, and the trend, and see a movement of 40 micron.

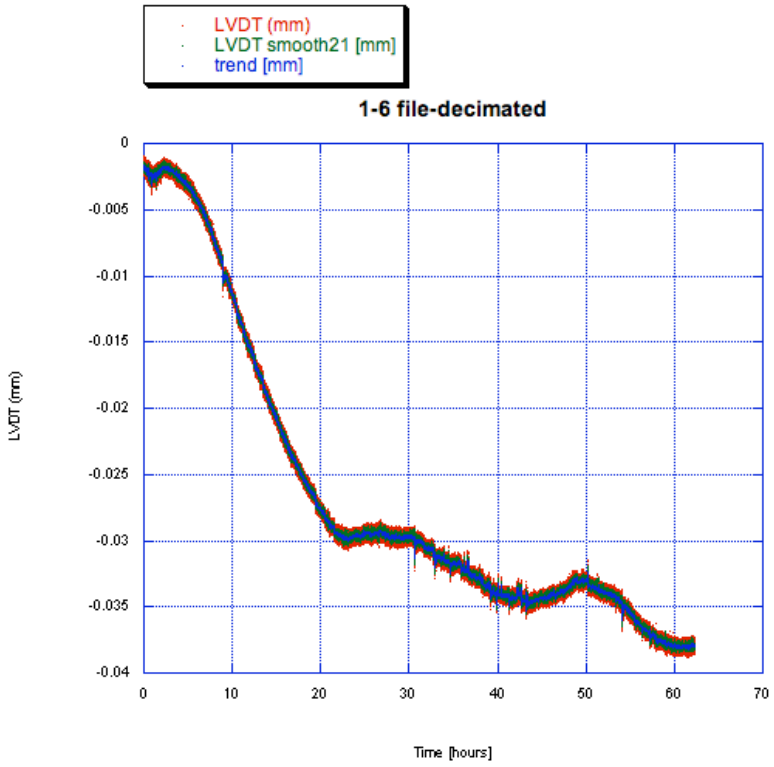

We explore the coil current:
We find that it drifts in a similar way, thus we average it further although we should have smoothed it before decimation.

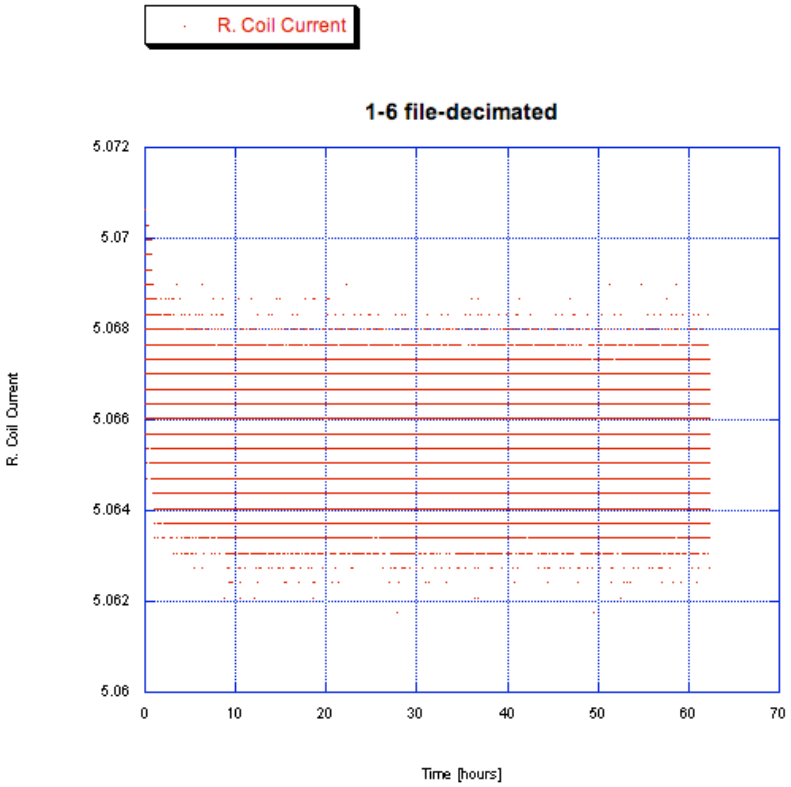

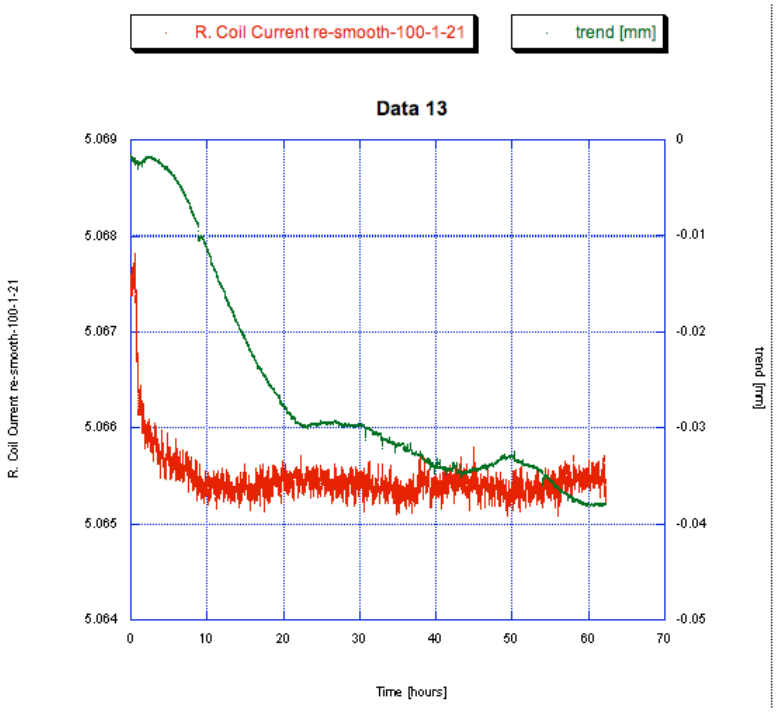

Although the current drift may have caused the position drift, it seems unlikely – the two drifts have probably different origins.

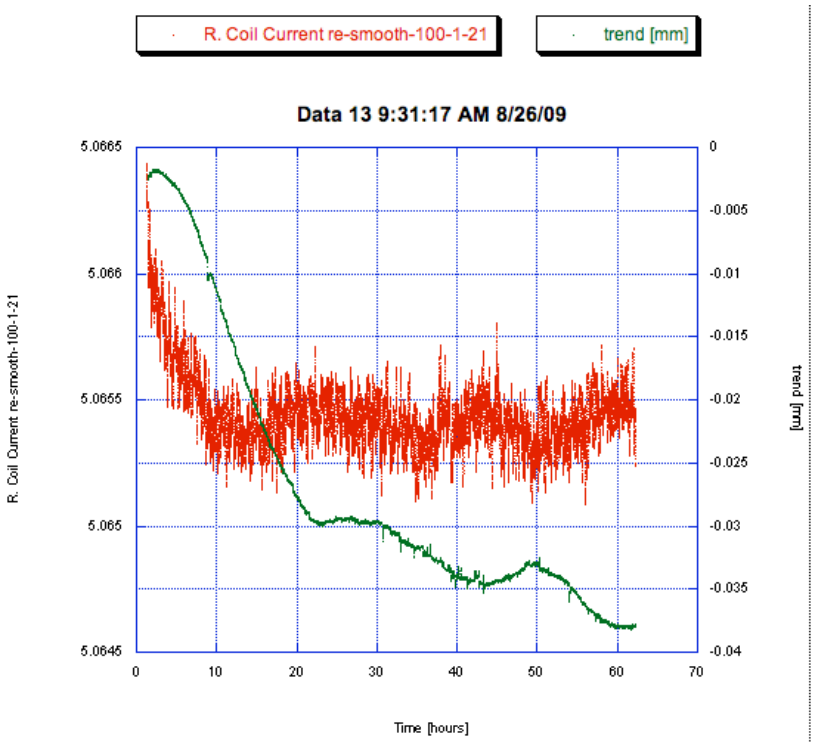

Finally, we look at the seismic re-excitation obtained by taking the absolute value of the flattened LVDT and averaging over several oscillation periods.

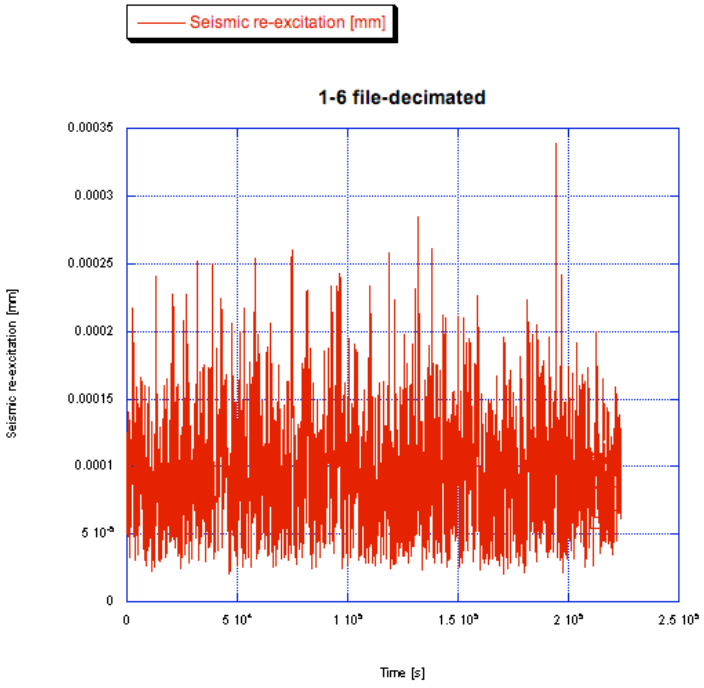

and histogramming it:

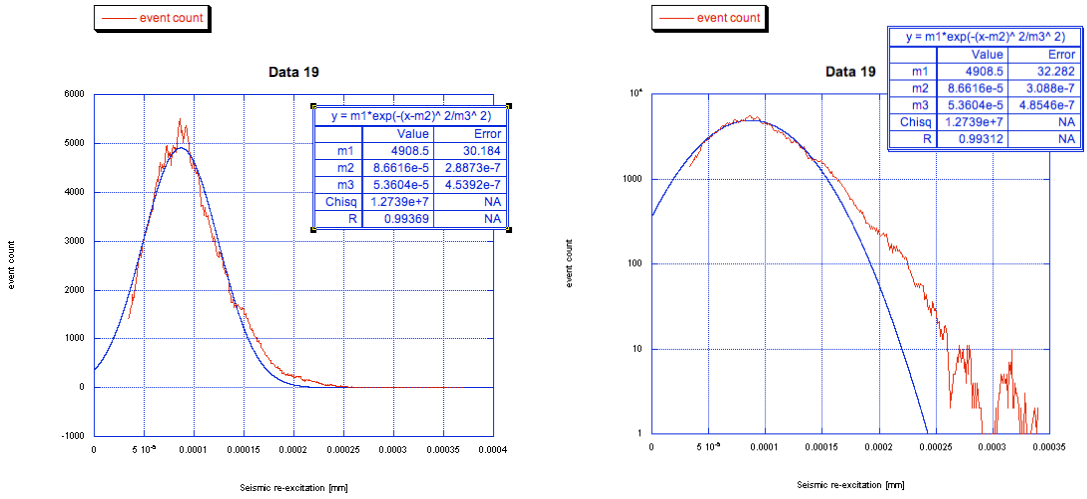

We get 87 nm (696 nanoradians) of seismic re-excitation at 60 mHz.
Taking into account the Q factor of the instrument (Q= τω/2 ~57; the following fit comes from the excitation at the beginning of the weekend data) and considering that the excitation amplitude should be the seismic excitation times the instrument's Q factor:

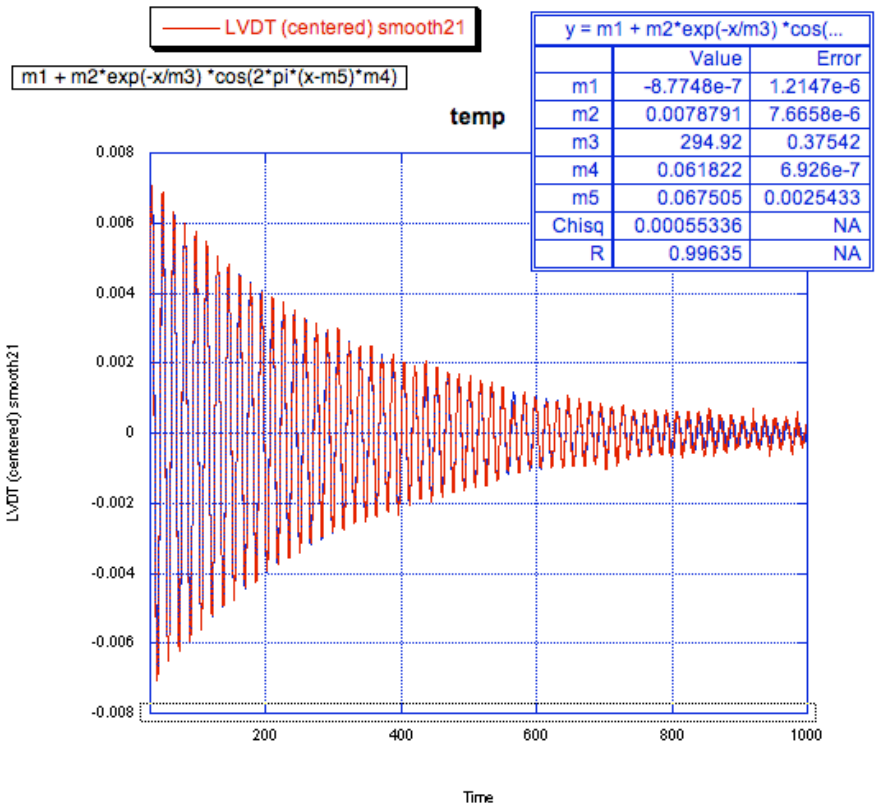

one gets an estimation of the upper limit of ground motion and ambient re-excitation (air currents) ~ 12 nanoradians of seismic noise at 60 mHz.

7 Conclusion and Future Work

By performing multiple tests on the tiltmeter system throughout the summer, we were able to characterize aspects of it and obtain quantitative measurements for the quality factor, hysteresis, and noise of the system. An undetermined error with the EMAS program resulted non-overlapping curves in the graphs of quality factor versus frequency. The lifetime and frequency of the ringdown depended on the amplitude of the oscillation, changing the quality factor of the system as it dampened. The hysteresis was shown to have a linear relationship with the amplitude of offset, but for small angles, there was barely any hysteresis, which is good. The system drifted over long periods of time, and a possible explanation of this could be due perhaps to thermal changes that affect the rubber base of the optical bench on which the tiltmeter currently resides. Step function analysis resulted in little noticeable hysteresis due to the ringdown oscillations of the tiltmeter. Noise analysis was done on data from two separate weekends to determine the sensitivity of the tiltmeter and its responses to seismic excitations, as well as the amount of electronic and digitations noise. The final noise level was determined to be on the order of 1e-6 radians per √Hz.

Future enhancements to the system include:
A new knife-edge made of wire-cut tungsten carbide coated in titanium nitrite
Testing done with a flexure blade
Improved actuator and feedback system, decreasing phase shift and delay
Replacement of LVDT with a better-precision optical sensor of the Michelson interferometer type